

NASA TECHNICAL NOTE



NASA TN D-6459

C.1

NASA TN D-6459



**LOAN COPY: RETURN
AFWL (DOUL)
KIRTLAND AFB, N. M.**

**INVESTIGATION OF TECHNIQUE FOR
CONDUCTING LANDING-IMPACT TESTS
AT SIMULATED PLANETARY GRAVITY**

*by Sandy M. Stubbs
Langley Research Center
Hampton, Va. 23365*



0133317

| | | | |
|---|---|--|---|
| 1. Report No. NASA TN D-6459 | 2. Government Accession No. | 3. Recipient's Catalog No. | |
| 4. Title and Subtitle INVESTIGATION OF TECHNIQUE FOR CONDUCTING LANDING-IMPACT TESTS AT SIMULATED PLANETARY GRAVITY | | 5. Report Date September 1971 | 6. Performing Organization Code |
| | | 8. Performing Organization Report No. L-7828 | 10. Work Unit No. 114-08-13-01 |
| 7. Author(s) Sandy M. Stubbs | 9. Performing Organization Name and Address NASA Langley Research Center Hampton, Va. 23365 | | 11. Contract or Grant No. |
| 12. Sponsoring Agency Name and Address National Aeronautics and Space Administration Washington, D.C. 20546 | | | 13. Type of Report and Period Covered Technical Note |
| 15. Supplementary Notes Film supplement L-1104 available on request | | | |
| 16. Abstract <p>In order to determine the suitability of landing systems for a Mars lander spacecraft, it is necessary to study the landing-gear structural loads, vehicle loads, motions, and stability at Mars gravity and at full size. There is need of a practical and economical technique for conducting full-scale Earth tests which would augment small-scale model tests and analytical investigations. Therefore, dynamic models have been used to develop and evaluate a technique for simulating planetary gravity during landing-impact tests. Results from landings at simulated Martian gravity show good correlation with results obtained during free-body Earth-gravity landings. Impact accelerations, time histories, and gear strokes obtained during hard-surface landings with the simulated Martian gravity and the Earth-gravity techniques are in good agreement. Model behavior and overturn characteristics compare favorably. Results indicate that the simulator technique could be used to conduct model and full-scale landing-impact investigations of planetary landers at reduced gravity.</p> | | | |
| 17. Key Words (Suggested by Author(s)) Simulated-gravity simulation Landing-impact tests | | 18. Distribution Statement Unclassified - Unlimited | |
| 19. Security Classif. (of this report) Unclassified | 20. Security Classif. (of this page) Unclassified | 21. No. of Pages 35 | 22. Price* \$3.00 |

INVESTIGATION OF TECHNIQUE
FOR CONDUCTING LANDING-IMPACT TESTS AT SIMULATED
PLANETARY GRAVITY

By Sandy M. Stubbs
Langley Research Center

SUMMARY

In order to determine the suitability of landing systems for a Mars lander spacecraft, it is necessary to study the landing-gear structural loads, vehicle loads, motions, and stability at Mars gravity and at full size. There is need of a practical and economical technique for conducting full-scale Earth tests which would augment small-scale model tests and analytical investigations. Therefore, dynamic models have been used to develop and evaluate a technique for simulating planetary gravity during landing-impact tests. Results from landings at simulated Martian gravity show good correlation with results obtained during free-body Earth-gravity landings. Impact accelerations, time histories, and gear strokes obtained during hard-surface landings with the simulated Martian gravity and the Earth-gravity techniques are in good agreement. Model behavior and overturn characteristics compare favorably. Results indicate that the simulator technique could be used to conduct model and full-scale landing-impact investigations of planetary landers at reduced gravity.

INTRODUCTION

The development of a spacecraft for landings on the Moon, Mars, or other planets requires full-scale testing to qualify the landing-gear structure and the primary body structure of the vehicle for the most severe loading condition that the spacecraft is expected to encounter. In order to maintain dynamic similarity during impact testing of the full-scale vehicle, it is necessary that the expected gravitational field be simulated. The effect of structural elasticity on the landing stability may also be evaluated in the simulated gravity environment of the planet. References 1 to 5 discuss several methods which can be used to simulate reduced gravitational force for prototype studies on Earth.

The purpose of the present investigation was to develop and evaluate a shock-cord suspension system for conducting landing-impact tests under simulated Martian gravity.

The landing forces and vehicle dynamics of a "Viking" type vehicle were also investigated. The Mars-gravity simulation technique, which employs a shock-cord support system, would offer a simple and economical method of obtaining landings with relatively high force response rates and with essentially free-body conditions.

Dynamic models (3/8-scale) of an early version of the Viking lander were tested to obtain data from a shock-cord simulation technique used to represent a planetary gravity that is less than that of the Earth. Results from this simulation technique were validated by comparison with those from free-body testing at Earth gravity. This paper presents data obtained from free-body tests and those obtained from simulated gravity tests.

Motion-picture film supplement L-1104 showing landing tests of the Mars-gravity and Earth-gravity models has been prepared and is available on loan. A request card form and a description of the film are included at the back of this paper.

SYMBOLS

The units used for the physical quantities defined in this paper are given both in the International System of Units (ref. 6) and in U.S. Customary Units. Appendix A presents factors relating these two systems of units. Measurements and calculations were made in the U.S. Customary Units.

| | |
|-------|---|
| A | area, m^2 (ft^2) |
| a | acceleration, m/sec^2 (ft/sec^2) |
| F | force, newtons (lbf) |
| g | gravity |
| I | inertia, $kg\cdot m^2$ ($slug\cdot ft^2$) |
| I_X | roll moment of inertia, $kg\cdot m^2$ ($slug\cdot ft^2$) |
| I_Y | pitch moment of inertia, $kg\cdot m^2$ ($slug\cdot ft^2$) |
| I_Z | yaw moment of inertia, $kg\cdot m^2$ ($slug\cdot ft^2$) |
| l | length, m (ft) |
| m | mass, kg (slugs) |

| | |
|-----------|---|
| t | time, sec |
| V_h | horizontal velocity, m/sec (ft/sec) |
| V_v | vertical velocity, m/sec (ft/sec) |
| v | velocity, m/sec (ft/sec) |
| X,Y,Z | body axes |
| β | gravitational ratio, Earth gravity/Mars gravity |
| λ | geometric model scale |
| σ | stress, N/m ² (lb/in ²) |

DESCRIPTION OF MODELS

Two 3/8-scale dynamic models of an early version of the "Viking" Mars lander spacecraft were used in the investigation. The model used on the reduced-gravity (Mars) simulator is designated as the Mars-gravity model. The model used as a control and tested as a free body in the Earth gravity is designated as the Earth-gravity model.

Scaling Laws

The scale relationships pertinent to the investigation are shown in table I, and parameters for the models and the full-scale vehicle are given in table II. Since it was desirable to use the same body structure for both models, the scale factor λ was the same for both Mars-gravity and Earth-gravity models. (See table I.) Force was varied as the cube of the scale factor (λ^3) for both models so that the same landing-gear shock absorber could be used on both models. The accelerations are the same for model and prototype in the Mars-gravity simulation test. For the Earth-gravity model, the accelerations vary as β , the gravitational ratio; thus, accelerations experienced by the Earth-gravity model were 8/3 times those which would occur on Mars or on the Mars-gravity simulator. With these three scale relationships fixed, other pertinent scale relationships follow from the laws of physics for dynamically scaled models.

For the purpose of comparing the Mars-gravity tests with the Earth-gravity tests, the gravitation ratio β is the only factor that determines the variation between the two test techniques. By using the chosen scaling relationships presented in table I, the only physical differences in the two models are the masses and the inertias.

Test Model Body

The general arrangement of the 3/8-scale models is shown in figure 1. The dimensional values given are full scale. Photographs of the basic model balanced for Mars-gravity and Earth-gravity tests are shown in figure 2. The primary structural frame is the same for both models and is made of welded aluminum tubing. The structural frame was made very light to allow a large amount of ballast weight for obtaining the correct masses, center-of-gravity location, and moments of inertia. Both models were ballasted so that all moments of inertia were within 3 percent of the desired value.

Two outrigger trusses mounted on the sides of the model near legs 2 and 3 (see fig. 1) provided attachment points for the shock-cord lift system. The attachment points were located on the transverse axis (Y-axis) equal distances from the center of gravity; thus, the lift forces had no effect on the stability of the vehicle.

Landing Gear

The location and designation of the landing gears and the individual struts are shown in figures 1 and 2. The primary struts were designated A, and the secondary struts were designated B and C. Each landing gear was an inverted tripod in which the primary strut served as the shock-absorbing element and the secondary struts served only as links having no shock-absorbing capability. The landing gear was free to move only in one plane with respect to the body axes.

A stiff, non-shock-absorbing footpad was attached to the bottom of the tripod by a ball joint which allowed the pad free pitching movements and 360° of rotation. All landing-gear components except the ball joints and sockets were made of 6061-T6 aluminum. The ball joints and sockets were made of 17-4 PH steel.

In changing the ballasting from the Earth-gravity model to the Mars-gravity model, care was taken that the unsprung mass of the landing gear was maintained in direct proportion to the total vehicle mass. The unsprung mass (9 percent of the total vehicle mass) consisted of the footpad, the main strut piston and piston rod, and half of the mass of the secondary struts. The additional unsprung mass was obtained by adding a torus of lead to the inside of each footpad (shown in fig. 2(a)).

Details of the primary strut assembly are shown in figure 3. The primary strut was a simple piston-cylinder arrangement. The cylinder had a centering rod held in place at the top of the strut by a thin disk. The centering rod, which positioned and held the crushable honeycomb elements, passed freely through a hole in the center of the piston head.

Four aluminum honeycomb, energy-absorbing cartridges (see fig. 3(b)) were used in each primary strut. These cartridges were crushed in compression (accordion-like column failure) by the landing loads imposed upon the telescoping landing-gear strut. The cartridges were separated by thin disks to insure proper crushing of each stage. Each cartridge was designed to crush at a predetermined force level which remained approximately constant during the strut stroke. A typical dynamic-force time history of the staged crush loads is shown in figure 3(a). The oscillograph record shown was from tests of an axially loaded strut and includes friction forces as well as honeycomb forces. The nominal crush loads for each stage are given in table II.

APPARATUS AND PROCEDURE

The acceleration due to gravity on Mars was assumed to be 3.69 m/sec^2 (12.1 ft/sec^2) and that on Earth to be 9.81 m/sec^2 (32.2 ft/sec^2) for this investigation. The investigation was conducted by launching the model as a shock-cord-supported body which simulated Mars-gravity conditions and also as a free body with Earth gravity acting.

Mars-Gravity Simulator

A sketch of the Mars-gravity simulation apparatus is shown in figure 4(a). Photographs of the test setup are shown in figure 5. An elastic suspension system with a shock cord was used to produce an upward force countering part of the Earth's gravitational force. Two shock cords were attached to the model by outrigger trusses mounted on the model in the horizontal plane of the vehicle center of gravity. The shock cords extended upward from the model to a cable which was run through a sheave. (See fig. 5(c).) The sheave was a low friction ball-bearing type and freely swiveled on a ball-bearing swivel. This suspension system allowed the vehicle to pitch, roll, and yaw simultaneously, the friction in the sheave being the only restriction. The sheave was attached to a line which extended upward to the trolley and was held by a cam cleat. The shock cords were attached to the model through force transducers shown in figure 5(b). The force transducers were used to monitor the shock-cord forces before and during the landing.

The model support line shown in figure 5(b) was used to lift and hold the model at the drop height required to produce the needed vertical velocity at impact. The model support line was attached to the model with an electromagnet. (See fig. 5(b).) Several attachment points were used so that the force of the model support line would always pass through the vehicle center of gravity for the various pitch attitudes. The line was extended upward to the trolley and held by another cam cleat.

The trolley was mounted on an overhead track to allow horizontal motion of the entire reduced-gravity system. The track was approximately 17 meters (55 feet) above the landing surface. Care was taken to construct the trolley light in weight and with low friction so it would follow vertically above the model.

The procedure used to obtain the correct simulation of the Mars-gravity force was as follows: The model was placed on the landing surface and the shock cord was stretched in tension by raising the swiveling sheave until the proper force ($5/8$ of the model weight) was registered by the force transducers. This procedure in effect gives a gravitation force of three-eighths of the model weight. The model was then attached to the model support line and raised to the drop height required to produce the necessary vertical velocity. In the raised or predrop position, the force in the shock cord was slightly less than the force required for Mars-gravity simulation. When the model was released, by turning off the power to the electromagnet, the force produced by the shock cord increased as the model fell and at impact was correct for Mars-gravity simulation.¹ It was necessary to make several preliminary runs to determine the drop height necessary to obtain the desired impact velocity.

The desired horizontal velocity was obtained by use of a falling mass to accelerate the model and trolley. A small tow cable was attached to the model so that its force acted in the plane of the vehicle center of gravity. The cable ran from the model, over a sheave, and down to the falling mass. (See fig. 4(a).) Another tow cable ran from the trolley, over a sheave, and down to the same falling mass. With the model held at the correct drop height needed for the desired vertical velocity and all acceleration cables taut, the model was pulled back to the prelaunch position shown by the dashed lines in figure 4(a). The prelaunch position was set so that the drop height of the falling mass was sufficient to produce the desired horizontal velocity of model and trolley. The model was held in the prelaunch position by a small cable attached to a release mechanism. When the release mechanism was triggered, the model and trolley were accelerated by the falling mass and moved forward. When the mass hit the ground, a microswitch was triggered to turn off the power to the electromagnet and allow the model to drop and attain the desired vertical velocity. The model acceleration cable was spring loaded at the model so that it would disconnect when the cable ceased to be taut. The trolley acceleration cable did not

¹The shock cord was found to have some undesirable characteristics. If the shock cord was stretched a given distance and held, the force in the shock cord decreased with time. Also, when the load was taken off, the shock cord did not immediately return to its original unstretched length. Temperature was also found to have an effect on the force in a stretched shock cord. A discussion of the elastic characteristic of rubber can be found in reference 7. In spite of these variations, consistent shock cord forces could be obtained if the shock cord was allowed to remain slack (no load) until a time immediately before the beginning of the test.

disconnect but did become slack when the falling mass hit the ground. The trolley acceleration cable was of low mass and had a negligible effect on the motions of the trolley.

Earth-Gravity Apparatus

A sketch of the Earth-gravity apparatus is shown in figure 4(b) and a photograph of the test setup is shown in figure 6. A pendulum was released from a predetermined height to produce the desired horizontal velocity. The model was released at the lowest point of the swing, and the predetermined free fall height gave the desired vertical velocity. The Earth-gravity tests were conducted in the Langley impacting structures facility.

Landing Surface and Friction Coefficient

The landing surface used for both the Mars-gravity and Earth-gravity tests was a relatively stiff wooden-frame-supported platform. Top surfaces of smooth plywood (figs. 5(a) and 5(b)) and sheet steel (fig. 6) were used in conjunction with various footpad coverings to give the desired friction coefficients. One end of the surface was raised to obtain various slope conditions. Only 0° and negative slopes were used in this investigation. Negative slopes are defined as the vehicle motion landing in the downhill direction.

The friction coefficients were determined by pulling a footpad along the landing surface. The footpad was loaded to approximately the mass of the Earth-gravity model. A weight pan was connected to the footpad by a light cord which passed over a low friction sheave. Sufficient mass was added to the weight pan to slide the footpad horizontally at a slow constant velocity once the static friction was overcome. The sliding velocity varied with friction coefficient and was estimated to be in the order of 0.6 m/sec (2 ft/sec) for the 0.1 coefficient and 0.03 m/sec (1 in./sec) for the 0.8 coefficient.

A coefficient of friction of approximately 0.1 was obtained by using a bare aluminum footpad on a smooth sheet of steel covered with light oil. A footpad covered with chamois skin on a smooth plywood surface was found to have a friction coefficient of about 0.5. A coefficient of approximately 0.8 was obtained by using a footpad covered with a thin rubber sheet on a smooth plywood surface.

Instrumentation and Data Reduction

Normal and longitudinal accelerations at the vehicle center of gravity were measured by using rigidly mounted piezoresistive strain-gage accelerometers. Primary strut stroke was measured on each landing gear by using three linear potentiometers. Strain gages were attached to all three struts of each landing gear and were calibrated to measure force. The signals from the accelerometers, potentiometers, and strain gages were transmitted through trailing cables to the recording equipment. The limiting flat frequency response of the accelerometers and potentiometers with the associated recording

equipment was 1000 Hz. The limiting response for the force measurements was 5000 Hz. The acceleration, stroke, and force data were recorded on frequency-modulated magnetic-tape recorders.

The acceleration and stroke data were passed through a 300 Hz low-pass filter to eliminate undesirable high frequency structural oscillations picked up by the accelerometers. The force data channels contained 880 Hz low-pass filters. After being filtered, all the data were digitized by using a sample rate of 2000 samples per second. The digital tapes were processed to obtain printouts and plots of the data.

Motion pictures (taken at 64 and 200 frames per second) were used to determine model landing attitudes and motions. A video camera and tape recorder were used to obtain an immediate review of the test conditions and landing behavior.

This instrumentation was common to both Mars-gravity and Earth-gravity tests. In addition, the Mars-gravity model had vertical-velocity and shock-cord force transducers and an additional normal accelerometer mounted just below the vehicle center of gravity. This accelerometer had a flat frequency response of 180 Hz. After proper signal conditioning, the data from these measurements were recorded directly on an oscillograph. The velocity transducer shown in figure 5(b) consisted of a small threaded drum attached to the shaft of a direct current generator. A low-stretch fine cord was wound on the drum and attached to the overhead trolley. As the vehicle fell, the cord turned the drum and generator, and generated dc voltage which was recorded directly on the oscillograph. The force transducers (one for each shock cord, see fig. 5(b)) were thin strain-gage tension links calibrated to measure force. The velocity and force transducers had flat frequency responses of 60 Hz.

Test Parameters

Sketches identifying vehicle axes, acceleration directions, attitudes, and flight path are shown in figure 7. Accelerations in the direction of the negative axes shown in figure 7 are considered as negative accelerations. Both vertical and horizontal velocities are treated as positive even though the horizontal velocity component is sometimes in the direction of the -Z-axis. All stroke measurements are treated as positive. The principal forces in the primary shock-absorbing struts are compression forces and are considered to be positive. In the secondary struts, however, tension forces are considered as positive and compression forces, as negative.

The procedure used for setting up the vehicle attitude for a test was as follows: With the model X-axis aligned with the gravity vector and leg 1 pointing in the direction of the horizontal velocity, the model was rolled about the X-axis to the desired roll attitude.

The model was then pitched about the Y-axis with leg 1 down being negative pitch and leg 1 up being positive pitch. Finally, the yaw angle was set with leg 2 down being right yaw and leg 2 up being left yaw.

Landings were made at touchdown pitch attitudes ranging from -14° to 18.5° . Nominal pitch conditions were -15° , 0° , and 15° . Roll attitudes were either 0° or 180° . All tests made with horizontal velocity were made at 180° roll (leg 1 trailing). Measurements show a scatter of yaw attitudes from 4° left yaw to 3° right yaw. Nominal vertical impact velocity was 7 m/sec (23 ft/sec) and nominal horizontal velocity was 0 or 2 m/sec (0 or 6 ft/sec). Landings were made on slopes of 0° , -20° , -25° , -30° , and -40° . Three different nominal friction coefficients were used in the investigation: 0.1, 0.5, and 0.8. It was intended that both Mars-gravity and Earth-gravity models be tested at identical landing conditions so that direct comparisons of results could be made. It was difficult to obtain identical runs for the two models, but most runs had only small differences in test conditions.

RESULTS AND DISCUSSION

The data obtained in the investigation are presented in tables III and IV. All values presented in this section are full scale unless otherwise indicated.

Mars-Gravity Simulation

In order to simulate a reduced gravity with the technique described in this paper, a constant upward or lift force must be applied to the vehicle to oppose part of the force of Earth's gravity. Figure 8 is a tracing of a typical oscillograph record showing the shock-cord forces compared with the force levels needed for Mars-gravity simulation. The sum of the forces of both shock cords when compared with the total lift force needed for Mars-gravity simulation was approximately 1 percent high at initial contact (time A). As the model continued downward, this difference increased to 6 percent high at time B. At time C, the vertical velocity of the model was stopped. The inertia of the shock cord, however, caused part of the cord to continue downward, and thus, relieved the load somewhat and gave a lift force that was 5 percent lower than the force needed for correct simulation. There was a surge in the shock cord due to its inertia that resulted in force oscillations until the run was completed.

An accelerometer trace shown in figure 8 was recorded as a reference for determining the time of initial contact. The vertical-velocity trace in figure 8 had a sine-wave oscillation due to elasticity of the fine cord that was used to turn the generator. It was necessary to fair the oscillations (fairing shown by the dashed line) in order to determine the velocity at impact.

The apparatus used in this investigation for simulating Mars gravity gave almost complete freedom of model angular motion in pitch, roll, and yaw. The overhead track allowed the vehicle to move freely fore and aft. The vehicle moved vertically with small changes in the gravity force. Small lateral motions were slightly restrained by the lateral component of force from the shock cord when the vehicle moved away from the center line of the overhead track. Thus, the simulator had five degrees of freedom with some slight limitations in the sixth degree.

Comparisons of Landing-Impact Loads

Acceleration and force time histories.- Comparisons of acceleration and force time histories for the Mars-gravity and Earth-gravity tests are shown in figure 9. The characteristics of the acceleration and force data for the two tests are very similar. There is a variation in the time, however, between Mars-gravity and Earth-gravity tests when legs 2 and 3 contact the landing surface and begin to load up. There is also a slight variation in the maximum acceleration between the Mars-gravity and Earth-gravity tests. These variations are attributed to the fact that the pitch attitude for the Mars-gravity test was actually 1° rather than the nominal 0° attitude given for the test conditions in figure 9. The premature contact of legs 2 and 3 of the Mars-gravity model is reflected in the normal-acceleration trace by the load falling off to zero at an earlier time than the Earth-gravity model.

The negative dips in the oscillograph traces of struts 1A, 2A, and 3A were erroneous signals and should be ignored. The negative dips were caused by bushings passing over the strain gages as the struts telescoped during crushing. The forces registered by the secondary struts give almost identical traces between Mars-gravity and Earth-gravity data although they are slightly out of phase. Overall, the time histories show good agreement between the Mars-gravity simulator tests and the Earth-gravity tests.

Maximum center-of-gravity accelerations.- Comparisons of maximum normal and longitudinal accelerations at the vehicle center of gravity plotted against touchdown pitch attitude for friction coefficients of approximately 0.05 to 0.15, 0.45 to 0.55, and 0.75 to 0.85 are shown in figure 10. The comparison indicates good agreement was obtained for the models using the two simulation techniques. The maximum normal acceleration was about 16g. Normal accelerations were more or less independent of the effects of friction coefficient except for the -13° attitude. When friction was increased for landings at a -13° attitude, the normal accelerations decreased from approximately -13g to about -8.5g. Maximum longitudinal accelerations had both positive and negative values as are shown in figure 10. As the friction coefficient was increased, the longitudinal acceleration increased and the highest positive and negative values plotted were 10g and -14g, respectively.

It should be noted that all the test data are given in tables III and IV, whereas only a limited number of runs are plotted in figure 10. The highest values of normal acceleration given in the tables are -20g and -22g for the Mars-gravity and Earth-gravity tests, respectively. The highest longitudinal accelerations are 10g and -14g for the Mars-gravity tests and 10g and -12g for the Earth-gravity tests when four-stage honeycomb elements were used in the shock-absorber legs. The entries given in the tables are values read from faired data. The fairing was done to eliminate the effects of structural vibrations that appear in the acceleration data and small amounts of electronic noise that occur occasionally on the force and stroke data.

Data showing correlation of maximum normal accelerations for Mars-gravity and Earth-gravity landings are presented in figure 11. All the normal acceleration data obtained while using the four-stage honeycomb elements are shown plotted against a line indicating exact correlation. The data indicate that good agreement was obtained between the Mars-gravity and Earth-gravity test methods. Some of the discrepancy occurs because the landing conditions for the Mars-gravity model were not all identical to those for the Earth-gravity model.

Maximum landing-gear forces.- Maximum forces measured in each strut of all three landing gears are presented in tables III and IV. Forces in the primary struts (1A, 2A, and 3A) are controlled and limited by the honeycomb elements of the shock absorbers. Forces in the secondary struts (B and C elements of each gear) indicate a trend toward higher values as landing surface friction is increased. The maximum force in the secondary struts for tests made with the four-stage honeycomb was about 50 kN (11 300 lbf).

Comparison of Landing Behavior

Landing-gear stroke.- The stroke time histories shown in figure 9(b) indicate good agreement between Mars-gravity and Earth-gravity data. The difference in impact time for legs 2 and 3 of the two models was due to slight differences in impact pitch attitude (as explained earlier). Figure 12 presents maximum stroke data for the three stroking struts under the same impact condition as the acceleration data presented in figure 10. The maximum stroke obtained was approximately 25 cm (10 inches). Agreement between the two test techniques was very good even though the strokes are sensitive to variations in shock-absorber element forces as well as slight differences in landing conditions.

Pitching motion and stability.- All runs made with the design force stroke characteristics represented by the four-stage honeycomb elements in shock-absorbing legs were quite stable with little tendency to pitch over even at high (0.8) friction coefficients tested on downhill slopes up to -30° and -40° . (See tables III and IV.) It was desirable to obtain a stability run in which the model would pitch up to turnover or near turnover attitude to see how well the Mars-gravity test technique agrees with the Earth-gravity tests. It was

found that the models would turn over if only the high force 36 kN (8000 lbf) honeycomb elements were used as shock absorbers in a landing on a -25° slope with a friction coefficient of 0.8. Landings made at a pitch attitude of -13° resulted in a rapid and decisive turnover, whereas landings made at 0° pitch were marginally stable, turnover occurring slowly and near the end of the slide-out. A comparison of pitch-time histories for both Mars-gravity and Earth-gravity models are shown in figure 13. The small sketches on the figure illustrate the position of the models with respect to the landing surface. The models were at 0° pitch attitude at initial contact. Legs 2 and 3 rotate downward and strike the surface at about 0.16 sec full-scale time. The footpad on leg 1 is free of the surface at the time legs 2 and 3 hit and the jolt of the second impact causes footpad 1 to rotate upward. While footpad 1 rotates upward, the models pitch back downward (illustrated by the dip in the pitch-time history curve) and hit on the edge of footpad 1 at a time of approximately 0.2 sec. The models then rebound off of leg 1 and pitch up slowly to a turnover position at a time of 0.8 to 1.0 sec. Both Mars-gravity and Earth-gravity models had a similar behavior throughout this unstable landing condition.

CONCLUDING REMARKS

A dynamic-model investigation has been conducted in order to develop and evaluate a technique for conducting landing-impact tests under the influence of simulated Martian gravity. Results of the tests at simulated Mars gravity show good correlation with results obtained during free-body Earth-gravity landing tests. Impact acceleration, time histories, and gear strokes experienced during hard-surface landings are in good agreement. Model impact behavior and overturn stability characteristics compare favorably. Although results and emphasis of the subject study are directed toward Mars gravity and "Viking" type spacecraft, the technique is applicable for other planetary landings at reduced gravity. Results from this investigation indicate that a simple and inexpensive elastic cord lift system with associated launching equipment would be a practical method for conducting a full-scale landing investigation of a Mars lander spacecraft.

Langley Research Center,
National Aeronautics and Space Administration,
Hampton, Va., July 9, 1971.

APPENDIX A

CONVERSION OF SI UNITS TO U.S. CUSTOMARY UNITS

Conversion factors for the units used herein are given in the following table:

| Physical quantity | SI Unit | Conversion factor (*) | U.S. Customary Unit |
|---------------------------|---|--------------------------|----------------------|
| Length | meters (m) | 39.37008 | in. |
| Area | meters ² (m ²) | 1550.0 | in ² |
| Mass | kilograms (kg) | 0.06852 | slug |
| Moment of inertia | kilogram-meters ² (kg-m ²) | 0.73756 | slug-ft ² |
| Velocity | meters/second (m/sec) | 3.28084 | ft/sec |
| Linear acceleration . . . | meters/second ² (m/sec ²) | 3.28084 | ft/sec ² |
| Force | newtons (N) | 0.22481 | lbf |

*Multiply value given in SI Unit by conversion factor to obtain equivalent value in U.S. Customary Unit.

Prefixes to indicate multiples of units are as follows:

| Prefix | Multiple |
|-----------|-----------|
| milli (m) | 10^{-3} |
| centi (c) | 10^{-2} |
| kilo (k) | 10^3 |

REFERENCES

1. O'Bryan, Thomas C.; and Hewes, Donald E.: Operational Features of the Langley Lunar Landing Research Facility. NASA TN D-3828, 1967.
2. Bellman, Donald R.; and Matranga, Gene J.: Design and Operational Characteristics of a Lunar-Landing Research Vehicle. NASA TN D-3023, 1965.
3. Carden, Huey D.; Herr, Robert W.; and Brooks, George W.: Technique for the Simulation of Lunar and Planetary Gravitational Fields Including Pilot Model Studies. NASA TN D-2415, 1964.
4. Hewes, Donald E.; and Spady, Amos A., Jr.: Evaluation of a Gravity-Simulation Technique for Studies of Man's Self-Loocomotion in Lunar Environment. NASA TN D-2176, 1964.
5. Blanchard, Ulysse J.: Model Investigation of Technique for Conducting Full-Scale Landing-Impact Tests at Simulated Lunar Gravity. NASA TN D-2586, 1965.
6. Comm. on Metric Practice: ASTM Metric Practice Guide. NBS Handbook 102, U.S. Dep. Com., Mar. 10, 1967.
7. Meyer, Kurt H.: Natural and Synthetic High Polymers. Interscience Publ., 1950.

TABLE I.- SCALE RELATIONSHIPS FOR TESTING MODELS ON EARTH
AT SIMULATED MARS GRAVITY CONDITIONS

Geometric model scale, $\lambda = 1/2.66$; gravitational ratio (Earth gravity/Mars gravity),
 $\beta = 2.66$. Note: For comparing the Mars-gravity tests with the Earth-gravity tests,
 $\lambda = 1$.

| Quantity | Mars prototype | Earth-gravity model scale factor | Mars-gravity model scale factor ($\beta = 1$) |
|---------------------|----------------|----------------------------------|---|
| *Length | l | λ | λ |
| *Force | F | λ^3 | λ^3 |
| *Acceleration . . . | a | β | 1 |
| Mass | m | λ^3/β | λ^3 |
| Area | A | λ^2 | λ^2 |
| Velocity | v | $\sqrt{\beta\lambda}$ | $\sqrt{\lambda}$ |
| Time | t | $\sqrt{\lambda/\beta}$ | $\sqrt{\lambda}$ |
| Inertia | I | λ^5/β | λ^5 |
| Stress | σ | λ | λ |

*Scale factors determining remaining scale relationships.

TABLE II.- PERTINENT MEASURED PARAMETERS OF 1/2.66-SCALE MODEL

| Parameter | Earth-gravity model | Mars-gravity model | Full-scale vehicle (Mars prototype) |
|---|---------------------|--------------------|-------------------------------------|
| Mass, kilograms (slugs) | 10 (0.7) | 27.1 (1.86) | 510 (35.0) |
| Moment of inertia, kg-m ² (slug-ft ²): | | | |
| I _X roll | 0.822 (0.606) | 2.186 (1.612) | 290 (214) |
| I _Y pitch | 0.544 (0.401) | 1.493 (1.101) | 197 (145) |
| I _Z yaw | 0.507 (0.374) | 1.33 (0.984) | 178 (131) |
| Body: | | | |
| Center-of-gravity height, m (in.) . . | 0.243 (9.57) | 0.243 (9.57) | 0.6467 (25.46) |
| Landing-gear radius, m (in.) | 0.5537 (21.80) | 0.5537 (21.80) | 1.473 (57.99) |
| Honeycomb-cartridge dynamic crush force, N (lbf) $\pm 10\%$: | | | |
| First stage | 471 (106) | 471 (106) | 9000 (2000) |
| Second stage | 707 (159) | 707 (159) | 13000 (3000) |
| Third stage | 943 (212) | 943 (212) | 18000 (4000) |
| Fourth stage | 1890 (425) | 1890 (425) | 36000 (8000) |

TABLE III.- MAXIMUM ACCELERATIONS, STROKES, AND FORCES FOR LANDINGS WITH MARS GRAVITY SIMULATION

[All values are full-scale (Mars prototype); R, right yaw (leg 2 down); L, left yaw (leg 3 down)]

(a) SI Units

| Mars run | Vertical velocity, m/sec | Horizontal velocity, m/sec | Landing attitude in - | | | Surface slope, deg | Friction coefficient, μ | Maximum acceleration at center of gravity, Earth g units | | Primary strut stroke, meters, for - | | | Maximum strut forces, kN, for - | | | | | | | | | Stability |
|---|--------------------------|----------------------------|-----------------------|-----------|----------|--------------------|-----------------------------|--|--------------|-------------------------------------|----------|----------|---------------------------------|----------|----------|----------|----------|----------|----------|----------|------------------|-----------|
| | | | Pitch, deg | Roll, deg | Yaw, deg | | | Normal | Longitudinal | Strut 1A | Strut 2A | Strut 3A | Gear 1 | | | Gear 2 | | | Gear 3 | | | |
| | | | | | | | | | | | | | Strut 1A | Strut 1B | Strut 1C | Strut 2A | Strut 2B | Strut 2C | Strut 3A | Strut 3B | Strut 3C | |
| 9, 13, 18, and 36 kN honeycomb elements used in shock-absorber legs | | | | | | | | | | | | | | | | | | | | | | |
| 1 | 7.16 | 0 | 1 | 0 | 1L | 0 | 0.1 | -17 | 3, -3 | 0.22 | 0.21 | 0.18 | 32 | -7, 9 | -22, 13 | 36 | -18, 13 | 13, -7 | 33 | -7, 13 | -16, 13 | |
| 2 | 6.80 | 0 | 1 | 0 | 0 | 0 | .5 | -20 | -5, 2 | .16 | .21 | .18 | 47 | 11, -5 | | 33 | -11, 13 | 9, -7 | 36 | -11, 2 | -4, 11 | |
| 3 | 7.47 | 0 | 1 | 0 | 1R | 0 | .8 | -17 | 5, -5 | .21 | .17 | .19 | 33 | -22, 2 | 20, -2 | 38 | -4, 5 | -11, 4 | 33 | 17, -7 | -16, 2 | |
| 4 | 6.86 | 2 | -12 | 180 | 1R | -20 | .1 | -13 | -4, 3 | .16 | .16 | .18 | 37 | -22, 16 | -14, 16 | 33 | 20, -22 | -18, 22 | 33 | -4, 12 | 11, -27 | |
| 5 | 7.25 | 2 | 3.5 | 180 | 0 | -20 | .1 | -13 | -4, 2 | .12 | .17 | .21 | 18 | -16, 7 | -9, 9 | 33 | 24, -24 | -20, 18 | 30 | -9, 13 | 14, -16 | |
| 6 | 7.47 | 2 | 15 | 180 | 0 | -20 | .1 | -14 | -5, 4 | .15 | .19 | .20 | 18 | -18, 13 | -10, 9 | 32 | 22, -30 | -13, 22 | 32 | -10, 13 | 18, -18 | |
| 7 | 7.13 | 2 | -13 | 180 | 3R | -20 | .5 | -11 | -10, 5 | .15 | .15 | .19 | 16 | -31, 11 | -17, 9 | 16 | 27, -9 | -44, 18 | 34 | -3, 33 | -27, 7 | |
| 8 | 7.04 | 2 | 1 | 180 | 2.5L | -20 | .5 | -12 | -3, 6 | .12 | .21 | .16 | 18 | -7, 7 | -16, 4 | 31 | 18, -27 | -8, 22 | 31 | -24, 22 | 27, -18 | |
| 9 | 7.28 | 2 | 18.5 | 180 | 1L | -20 | .5 | -16 | -3, 5 | .15 | .20 | .18 | 31 | -11, 10 | -9, 16 | 33 | 11, -18 | -7, 16 | 31 | -16, 24 | 13, -24 | |
| 10 | 6.71 | 2 | -13 | 180 | 1R | -20 | .8 | -8 | -14, 8 | .09 | .15 | .16 | 16 | -42, 4 | -38, 4 | 18 | -42, 4 | 22, -4 | 27 | -13, 24 | 16, -40 | |
| 11 | 7.50 | 2 | 3.5 | 180 | 0 | -20 | .8 | -13 | -4, 10 | .12 | .19 | .19 | 18 | -16, 18 | -13, 7 | 33 | 27, -29 | -27, 42 | 33 | -13, 40 | 24, -22 | |
| 12 | 7.68 | 2 | 17 | 180 | 1R | -20 | .8 | -13 | -3, 9 | .14 | .18 | .25 | 14 | -13, 13 | -9, 11 | 33 | 16, -24 | -11, 33 | 41 | -11, 38 | 13, -27 | |
| 13 | 6.77 | 2 | -10 | 180 | 1L | -30 | .8 | -6 | -10, 6 | .08 | .14 | .12 | 20 | 7, -24 | -36, 2 | 17 | -29, 0 | 31, -13 | 14 | -2, 21 | 7, -38 | |
| 14 | 7.04 | 2 | 3 | 180 | 2L | -30 | .8 | -10 | -4, 9 | .09 | .19 | .16 | 18 | -11, 11 | -16, 7 | 33 | 9, -36 | -2, 42 | 34 | | 16, -29 | |
| 15 | 7.01 | 2 | 2.5 | 180 | 2L | -40 | .8 | -7 | -5, 8 | .09 | .17 | .14 | 16 | -13, 4 | -13, 7 | 33 | 10, -44 | -4, 31 | 20 | -13, 29 | 16, -39 | |
| Only 36 kN honeycomb element used in shock-absorber legs | | | | | | | | | | | | | | | | | | | | | | |
| 16 | 6.92 | 2 | -13 | 180 | 0.5R | -25 | 0.8 | -18 | -15, 16 | 0.03 | 0.05 | 0.05 | 41 | -42, 0 | -33, 0 | 40 | -53, 0 | 27, 0 | 39 | 38, 0 | -53, 7 Turnover | |
| 17 | 7.16 | 2 | 0 | 180 | 2L | -25 | .8 | -12 | -6, 10 | .03 | .07 | .04 | 36 | -11, 11 | -11, 13 | 40 | 22, -44 | 31, 0 | 39 | -11, 38 | 31, -38 Turnover | |
| 18 | 7.56 | 2 | 17 | 180 | 0 | -25 | .8 | -17 | -6, 11 | .03 | .07 | .04 | 38 | -13, 22 | -7, 17 | 40 | 40, -31 | -6, 31 | 41 | -4, 29 | 36, -31 | |

TABLE III.- MAXIMUM ACCELERATIONS, STROKES, AND FORCES FOR LANDINGS WITH MARS GRAVITY SIMULATION - Concluded

(b) U.S. Customary Units

| Mars run | Vertical velocity, ft/sec | Horizontal velocity, ft/sec | Landing attitude in - | | | Surface slope, deg | Friction coefficient, μ | Maximum acceleration at center of gravity, Earth g units | | Primary strut stroke, in., for - | | | Maximum strut forces, thousand pounds, for - | | | | | | Stability | | | |
|---|---------------------------|-----------------------------|-----------------------|-----------|----------|--------------------|-----------------------------|--|--------------|----------------------------------|----------|----------|--|-----------|-----------|----------|------------|------------|-----------|-----------|------------|----------|
| | | | Pitch, deg | Roll, deg | Yaw, deg | | | Normal | Longitudinal | Strut 1A | Strut 2A | Strut 3A | Gear 1 | | Gear 2 | | Gear 3 | | | | | |
| | | | | | | | | | | | | | Strut 1A | Strut 1B | Strut 1C | Strut 2A | Strut 2B | Strut 2C | | Strut 3A | Strut 3B | Strut 3C |
| 2000, 3000, 4000, and 8000 lbf honeycomb elements used in shock-absorber legs | | | | | | | | | | | | | | | | | | | | | | |
| 1 | 23.5 | 0 | 1 | 0 | 1L | 0 | 0.1 | -17 | 3, -3 | 8.7 | 8.1 | 7.1 | 7.2 | -7.5, 2.0 | -5.0, 3.0 | 8.0 | -4.0, 5.0 | 3.0, -1.5 | 7.5 | -1.5, 3.0 | -3.5, 3.0 | |
| 2 | 22.3 | 0 | 1 | 0 | 0 | 0 | .5 | -20 | -5, 2 | 6.5 | 8.2 | 7.0 | 10.5 | 2.5, -1.2 | | 7.5 | -2.5, 3.0 | 2.0, -1.5 | 8.0 | -2.5, 0.5 | -1.0, 2.5 | |
| 3 | 24.5 | 0 | 1 | 0 | 1R | 0 | .8 | -17 | 5, -5 | 8.3 | 6.6 | 7.4 | 7.5 | -5.0, 0.5 | 4.5, -0.5 | 8.5 | -1.0, 1.2 | -2.5, 1.0 | 7.5 | 3.8, -1.5 | -3.5, 0.5 | |
| 4 | 22.5 | 6 | -12 | 180 | 1R | -20 | .1 | -13 | -4, 3 | 6.4 | 6.3 | 7.0 | 8.3 | -5.0, 3.5 | -3.2, 3.5 | 7.5 | 4.5, -5.0 | -4.0, 5.0 | 7.5 | -1.0, 2.8 | 2.5, -6.0 | |
| 5 | 23.8 | 6 | 3.5 | 180 | 0 | -20 | .1 | -13 | -4, 2 | 4.9 | 6.8 | 8.4 | 4.0 | -3.5, 1.5 | -2.0, 2.0 | 7.5 | 5.5, -5.5 | -4.5, 4.0 | 6.7 | -2.0, 3.0 | 3.2, -3.5 | |
| 6 | 24.5 | 6 | 15 | 180 | 0 | -20 | .1 | -14 | -5, 4 | 5.8 | 7.3 | 7.9 | 4.0 | -4.0, 3.0 | -2.3, 2.0 | 7.3 | 5.0, -6.7 | -3.0, 5.0 | 7.3 | -2.2, 3.0 | 4.0, -4.0 | |
| 7 | 23.4 | 6 | -13 | 180 | 3R | -20 | .5 | -11 | -10, 5 | 5.8 | 5.8 | 7.3 | 3.7 | -7.0, 2.5 | -4.0, 2.0 | 3.7 | 6.0, -2.0 | -10.0, 4.0 | 7.7 | -0.7, 7.5 | -6.0, 1.5 | |
| 8 | 23.1 | 6 | 1 | 180 | 2.5L | -20 | .5 | -12 | -3, 6 | 4.6 | 8.4 | 6.3 | 4.0 | -1.5, 1.5 | -3.5, 1.0 | 7.0 | 4.0, -6.0 | -1.7, 5.0 | 7.0 | -5.5, 5.0 | 6.0, -4.0 | |
| 9 | 23.9 | 6 | 18.5 | 180 | 1L | -20 | .5 | -16 | -3, 5 | 6.1 | 7.8 | 7.0 | 7.0 | -2.5, 2.2 | -2.0, 3.5 | 7.5 | 2.5, -4.0 | -1.5, 3.5 | 7.0 | -3.5, 5.5 | 3.0, -5.5 | |
| 10 | 22.0 | 6 | -13 | 180 | 1R | -20 | .8 | -8 | -14, 8 | 3.4 | 5.8 | 6.4 | 3.7 | -9.5, 1.0 | -8.5, 1.0 | 4.0 | -9.2, 1.0 | 5.0, -1.0 | 6.0 | -3.0, 5.5 | 3.5, -9.0 | |
| 11 | 24.6 | 6 | 3.5 | 180 | 0 | -20 | .8 | -13 | -4, 10 | 4.8 | 7.3 | 7.4 | 4.0 | -3.5, 4.0 | -3.0, 1.5 | 7.5 | 6.0, -6.5 | -6.0, 9.5 | 7.5 | -3.0, 9.0 | 5.5, -5.0 | |
| 12 | 25.2 | 6 | 17 | 180 | 1R | -20 | .8 | -13 | -3, 9 | 5.6 | 7.0 | 9.7 | 3.2 | -3.0, 3.0 | -2.0, 2.5 | 7.5 | 3.5, -5.5 | -2.5, 7.5 | 9.3 | -2.5, 8.5 | 3.0, -6.0 | |
| 13 | 22.2 | 6 | -10 | 180 | 1L | -30 | .8 | -6 | -10, 6 | 3.0 | 5.6 | 4.9 | 4.4 | 1.5, -5.5 | -8.0, 0.5 | 3.9 | -6.5, 0 | 7.0, -3.0 | 3.2 | -0.5, 4.7 | 1.5, -8.5 | |
| 14 | 23.1 | 6 | 3 | 180 | 2L | -30 | .8 | -10 | -4, 9 | 3.6 | 7.5 | 6.4 | 4.0 | -2.5, 2.5 | -3.5, 1.5 | 7.5 | 2.0, -8.0 | -0.5, 9.5 | 7.7 | | 3.5, -6.5 | |
| 15 | 23.0 | 6 | 2.5 | 180 | 2L | -40 | .8 | -7 | -5, 8 | 3.4 | 6.5 | 5.4 | 3.5 | -3.0, 1.0 | -3.0, 1.5 | 7.5 | 2.3, -10.0 | -1.0, 7.0 | 4.5 | -3.0, 6.5 | 3.5, -8.5 | |
| Only 8000 lbf honeycomb element used in shock-absorber legs | | | | | | | | | | | | | | | | | | | | | | |
| 16 | 22.7 | 6 | -13 | 180 | 0.5R | -25 | 0.8 | -18 | -15, 16 | 1.2 | 2.0 | 2.1 | 9.3 | -9.5, 0 | -7.5, 0 | 9.0 | -12.0, 0 | 6.0, 0 | 8.7 | 8.5, 0 | -12.0, 1.5 | Turnover |
| 17 | 23.5 | 6 | 0 | 180 | 2L | -25 | .8 | -12 | -6, 10 | 1.2 | 2.9 | 1.5 | 8.2 | -2.5, 2.5 | -2.5, 3.0 | 9.0 | 5.0, -10.0 | 7.0, 0 | 8.7 | -2.5, 8.5 | 7.0, -8.5 | Turnover |
| 18 | 24.8 | 6 | 17 | 180 | 0 | -25 | .8 | -17 | -6, 11 | 1.3 | 2.6 | 1.4 | 8.5 | -3.0, 5.0 | -1.5, 4.0 | 9.0 | 9.0, -7.0 | -1.4, 7.0 | 9.3 | -1.0, 6.5 | 8.0, -7.0 | |

TABLE IV.- MAXIMUM ACCELERATIONS, STROKES, AND FORCES FOR LANDINGS WITH EARTH GRAVITY

[All values are full-scale (Mars prototype); R, right yaw (leg 2 down); L, left yaw (leg 3 down)]

(a) SI Units

| Earth run | Vertical velocity, m/sec | Horizontal velocity, m/sec | Landing attitude in - | | | Surface slope, deg | Friction coefficient, μ | Maximum acceleration at center of gravity, Earth g units | | Primary strut stroke, meters, for - | | | Maximum strut forces, kN, for - | | | | | | Stability | | | |
|---|--------------------------|----------------------------|-----------------------|-----------|----------|--------------------|-----------------------------|--|--------------|-------------------------------------|----------|----------|---------------------------------|----------|----------|----------|----------|----------|-----------|----------|----------|----------|
| | | | Pitch, deg | Roll, deg | Yaw, deg | | | Normal | Longitudinal | Strut 1A | Strut 2A | Strut 3A | Gear 1 | | Gear 2 | | Gear 3 | | | | | |
| | | | | | | | | | | | | | Strut 1A | Strut 1B | Strut 1C | Strut 2A | Strut 2B | Strut 2C | | Strut 3A | Strut 3B | Strut 3C |
| 9, 13, 18, and 36 kN honeycomb elements used in shock-absorber legs | | | | | | | | | | | | | | | | | | | | | | |
| 1 | 7.0 | 0 | 0.5 | 180 | 0.5R | 0 | 0.1 | -22 | -4, 2 | 0.19 | 0.16 | 0.21 | 38 | -18, 13 | 10, 0 | 38 | -18, 13 | -16, 12 | 38 | -9, 13 | -11, 11 | |
| 2 | 7.0 | 0 | 1 | 180 | 1R | 0 | .5 | -21 | 2, -3 | .21 | .17 | .18 | 38 | -10, 6 | 8, -3 | 33 | -13, 6 | -20, 9 | 36 | | -16, 7 | |
| 3 | 7.0 | 0 | 0 | 180 | 0 | 0 | .8 | -20 | -4, 2 | .19 | .18 | .20 | 31 | -20, 4 | -16, 9 | 36 | -4, 4 | -16, 4 | 37 | -9, 4 | -13, 7 | |
| 4 | 6.92 | 2 | -12 | 180 | 2R | -20 | .1 | -13 | -9, 3 | .15 | .15 | .17 | 18 | -27, 9 | -22, 18 | 27 | 16, -20 | -9, 12 | 37 | | 9, -25 | |
| 5 | 7.10 | 2 | 0 | 180 | 1L | -20 | .1 | -16 | -5, 2 | .15 | .18 | .16 | 39 | -16, 12 | -13, 13 | 33 | -18, 9 | -13, 13 | 40 | -9, 13 | 16, -27 | |
| 6 | 7.13 | 2 | 13 | 180 | 2R | -20 | .1 | -16 | -4, 2 | .13 | .15 | .19 | 16 | -9, 9 | -9, 7 | 39 | 16, -18 | -9, 13 | 36 | | 16, -18 | |
| 7 | 6.92 | 2 | -12.5 | 180 | 1L | -20 | .5 | -12 | -10, 6 | .13 | .17 | .15 | 15 | -29, 7 | -29, 7 | 42 | 11, -31 | -2, 22 | 20 | -7, 16 | 16, -22 | |
| 8 | 7.10 | 2 | 0 | 180 | 2.5L | -20 | .5 | -12 | -5, 5 | .13 | .18 | .15 | 18 | -9, 7 | -9, 7 | 36 | 16, -23 | -7, 27 | 22 | -13, 16 | 22, -16 | |
| 9 | 7.22 | 2 | 13 | 180 | 0 | -20 | .5 | -15 | -4, 6 | .12 | .19 | .17 | 16 | -9, 4 | -9, 9 | 37 | 20, -14 | -13, 27 | 36 | -13, 22 | 20, -14 | |
| 10 | 7.01 | 2 | -14 | 180 | 3.5L | -20 | .8 | -9 | -12, 7 | .12 | .19 | .12 | 16 | -27, 7 | -34, 7 | 31 | 9, -33 | -2, 25 | 18 | -22, 20 | 20, -20 | |
| 11 | 7.19 | 2 | 1.5 | 180 | 0 | -20 | .8 | -15 | -5, 9 | .12 | .19 | .18 | 16 | -18, 9 | -18, 9 | 43 | 22, -27 | -16, 31 | 33 | -10, 27 | 18, -16 | |
| 12 | 7.28 | 2 | 11 | 180 | 4L | -20 | .8 | -15 | -3, 10 | .11 | .21 | .16 | 15 | 11, -2 | -17, 12 | 36 | 20, -38 | -7, 21 | 33 | -16, 36 | 20, -25 | |
| 13 | 6.59 | 2 | -12.5 | 180 | 2R | -30 | .8 | -7 | -8, 6 | .08 | .11 | .15 | 13 | -22, 4 | -20, 4 | 12 | 9, -31 | -4, 22 | 30 | 50, 0 | -40, 4 | |
| 14 | 6.98 | 2 | 0 | 180 | 0 | -30 | .8 | -9 | -3, 7 | .09 | .15 | .15 | 13 | -11, 7 | -9, 4 | 25 | 14, -27 | -7, 22 | 29 | | 13, -29 | |
| 15 | 7.13 | 2 | 0 | 180 | 1R | -40 | .8 | -8 | -4, 8 | .08 | .12 | .16 | 16 | -13, 4 | -11, 4 | 16 | 11, -36 | -7, 25 | 31 | -2, 27 | 9, -42 | |
| Only 36 kN honeycomb element used in shock-absorber legs | | | | | | | | | | | | | | | | | | | | | | |
| 16 | 7.04 | 2 | -12.5 | 180 | 2R | -25 | 0.8 | -11 | -11, 10 | 0.02 | 0.03 | 0.06 | 42 | -29, 8 | -25, 4 | 39 | 9, -49 | -8, 38 | 36 | 49, 0 | -58, 4 | Turnover |
| 17 | 7.22 | 2 | 1 | 180 | 0 | -25 | .8 | -15 | -5, 10 | .03 | .05 | .07 | 38 | 13, -11 | 10, -11 | 36 | 31, -36 | -18, 38 | 40 | 58, -10 | 31, -36 | Turnover |

TABLE IV.- MAXIMUM ACCELERATIONS, STROKES, AND FORCES FOR LANDINGS WITH EARTH GRAVITY - Concluded

(b) U.S. Customary Units

| Earth run | Vertical velocity, ft/sec | Horizontal velocity, ft/sec | Landing attitude in - | | | Surface slope, deg | Friction coefficient, μ | Maximum acceleration at center of gravity, Earth g units | | Primary strut stroke, in., for - | | | Maximum strut forces, thousand pounds, for - | | | | | | | | | Stability |
|---|---------------------------|-----------------------------|-----------------------|-----------|----------|--------------------|-----------------------------|--|--------------|----------------------------------|----------|----------|--|-----------|-----------|----------|------------|-----------|----------|------------|------------|-----------|
| | | | Pitch, deg | Roll, deg | Yaw, deg | | | Normal | Longitudinal | Strut 1A | Strut 2A | Strut 3A | Gear 1 | | | Gear 2 | | | Gear 3 | | | |
| | | | | | | | | | | | | | Strut 1A | Strut 1B | Strut 1C | Strut 2A | Strut 2B | Strut 2C | Strut 3A | Strut 3B | Strut 3C | |
| 2000, 3000, 4000, and 8000 lbf honeycomb elements used in shock-absorber legs | | | | | | | | | | | | | | | | | | | | | | |
| 1 | 23 | 0 | 0.5 | 180 | 0.5R | 0 | 0.1 | -22 | -4, 2 | 7.4 | 6.4 | 8.3 | 8.5 | -4.0, 3.0 | 2.2, 0 | 8.5 | -4.0, 3.0 | -3.5, 2.8 | 8.5 | -2.0, 3.0 | -2.5, 2.5 | |
| 2 | 23 | 0 | 1 | 180 | 1R | 0 | .5 | -21 | 2, -3 | 8.1 | 6.7 | 7.0 | 8.5 | -2.3, 1.3 | 1.8, -0.7 | 7.5 | -3.0, 1.4 | -4.5, 2.0 | 8.2 | | -3.5, 1.5 | |
| 3 | 23 | 0 | 0 | 180 | 0 | 0 | .8 | -20 | -4, 2 | 7.6 | 7.0 | 7.7 | 7.0 | -4.4, 1.0 | -3.5, 2.0 | 8.0 | -1.0, 1.0 | -3.5, 1.0 | 8.3 | -2.0, 1.0 | -3.0, 1.5 | |
| 4 | 22.7 | 6 | -12 | 180 | 2R | -20 | .1 | -13 | -9, 3 | 5.8 | 5.8 | 6.8 | 4.0 | -6.0, 2.0 | -5.0, 4.0 | 6.0 | 3.5, -4.5 | -2.0, 2.8 | 8.4 | | 2.0, -5.5 | |
| 5 | 23.3 | 6 | 0 | 180 | 1L | -20 | .1 | -16 | -5, 2 | 6.0 | 7.0 | 6.2 | 8.8 | -3.5, 2.8 | -3.0, 3.0 | 7.5 | -4.0, 2.0 | -3.0, 3.0 | 9.0 | -2.0, 3.0 | 3.5, -6.0 | |
| 6 | 23.4 | 6 | 13 | 180 | 2R | -20 | .1 | -16 | -4, 2 | 5.2 | 6.1 | 7.6 | 3.6 | -2.0, 2.0 | -2.0, 1.5 | 8.7 | 3.5, -4.0 | -2.0, 3.0 | 8.0 | | 3.5, -4.0 | |
| 7 | 22.7 | 6 | -12.5 | 180 | 1L | -20 | .5 | -12 | -10, 6 | 5.1 | 6.5 | 5.9 | 3.4 | -6.5, 1.5 | -6.5, 1.5 | 9.5 | 2.5, -7.0 | -0.5, 5.0 | 4.5 | -1.5, 3.5 | 3.7, -5.0 | |
| 8 | 23.3 | 6 | 0 | 180 | 2.5L | -20 | .5 | -12 | -5, 5 | 5.2 | 7.2 | 6.1 | 4.0 | -2.0, 1.5 | -2.0, 1.5 | 8.0 | 3.7, -5.2 | -1.5, 6.0 | 5.0 | -3.0, 3.5 | 5.0, -3.5 | |
| 9 | 23.7 | 6 | 13 | 180 | 0 | -20 | .5 | -15 | -4, 6 | 4.8 | 7.6 | 6.8 | 3.5 | -2.0, 1.0 | -2.0, 2.0 | 8.3 | 4.5, -3.2 | -3.0, 6.0 | 8.0 | -3.0, 5.0 | 4.5, -3.2 | |
| 10 | 23.0 | 6 | -14 | 180 | 3.5L | -20 | .8 | -9 | -12, 7 | 4.6 | 7.3 | 4.9 | 3.5 | -6.0, 1.5 | -7.7, 1.5 | 7.0 | 2.0, -7.5 | -0.5, 5.5 | 4.0 | -5.0, 4.5 | 4.5, -4.5 | |
| 11 | 23.6 | 6 | -1.5 | 180 | 0 | -20 | .8 | -15 | -5, 9 | 4.7 | 6.8 | 7.0 | 3.5 | -4.0, 2.0 | -4.0, 2.0 | 9.7 | 5.0, -6.0 | -3.5, 7.0 | 7.5 | -2.3, 6.0 | 4.0, -3.5 | |
| 12 | 23.9 | 6 | 11 | 180 | 4L | -20 | .8 | -15 | -3, 10 | 4.3 | 8.1 | 6.2 | 3.3 | 2.5, -0.5 | -3.8, 2.8 | 8.2 | 4.5, -8.5 | -1.5, 4.8 | 7.5 | -3.5, 8.2 | 4.5, -5.5 | |
| 13 | 22.5 | 6 | -12.5 | 180 | 2R | -30 | .8 | -7 | -8, 6 | 3.3 | 4.5 | 6.1 | 3.0 | -5.0, 1.0 | -4.5, 1.0 | 2.7 | 2.0, -7.0 | -1.0, 5.0 | 6.7 | 11.3, 0 | -9.0, 1.0 | |
| 14 | 22.9 | 6 | 0 | 180 | 0 | -30 | .8 | -9 | -3, 7 | 3.7 | 5.8 | 5.9 | 3.0 | -2.5, 1.5 | -2.0, 1.0 | 5.5 | 3.2, -6.0 | -1.5, 5.0 | 6.5 | | 3.0, -6.5 | |
| 15 | 23.4 | 6 | 0 | 180 | 1R | -40 | .8 | -8 | -4, 8 | 3.1 | 4.9 | 6.2 | 3.5 | -3.0, 1.0 | -2.5, 1.0 | 3.6 | 2.6, -8.0 | -1.5, 5.5 | 7.0 | -0.5, 6.0 | 2.0, -9.5 | |
| Only 8000 lbf honeycomb element used in shock-absorber legs | | | | | | | | | | | | | | | | | | | | | | |
| 16 | 23.1 | 6 | -12.5 | 180 | 2R | -25 | 0.8 | -11 | -11, 10 | 0.8 | 1.2 | 2.2 | 9.5 | -6.5, 1.7 | -5.5, 1.0 | 8.7 | 2.0, -11.0 | -1.8, 8.5 | 8.2 | 11.0, 0 | -13.0, 1.0 | Turnover |
| 17 | 23.7 | 6 | 1 | 180 | 0 | -25 | .8 | -15 | -5, 10 | 1.2 | 1.9 | 2.8 | 8.5 | 3.0, -2.5 | 2.2, -2.5 | 8.0 | 7.0, -8.0 | -4.0, 8.5 | 9.0 | 13.0, -2.2 | 7.0, -8.2 | Turnover |

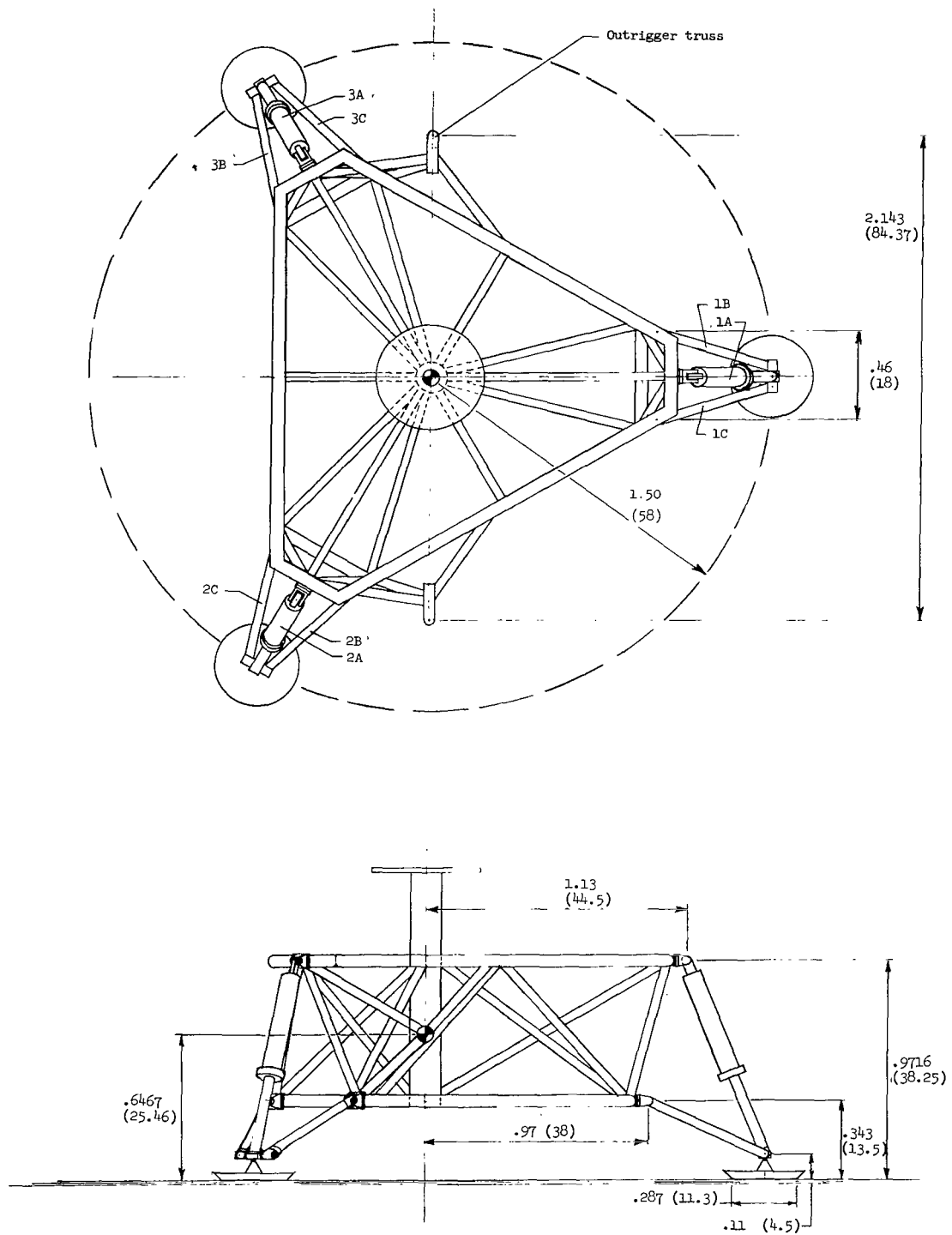
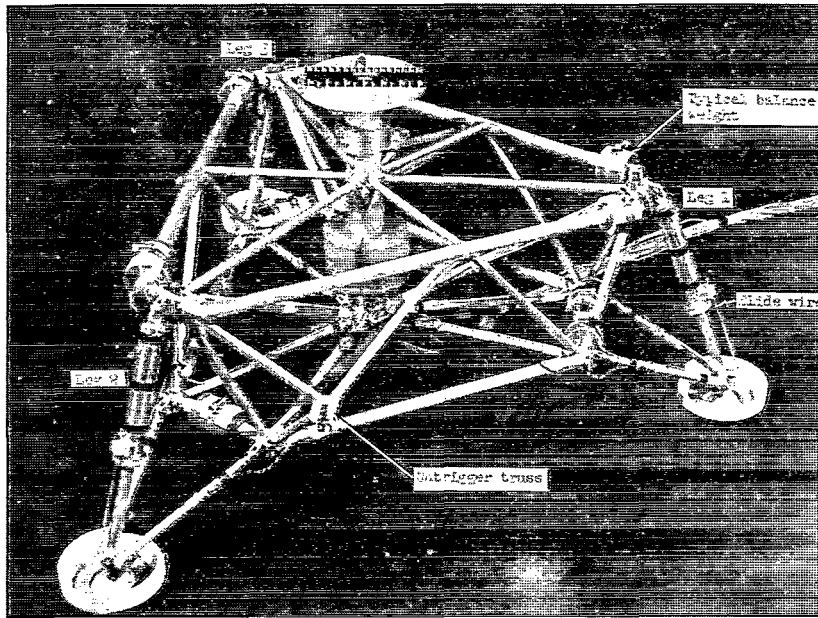
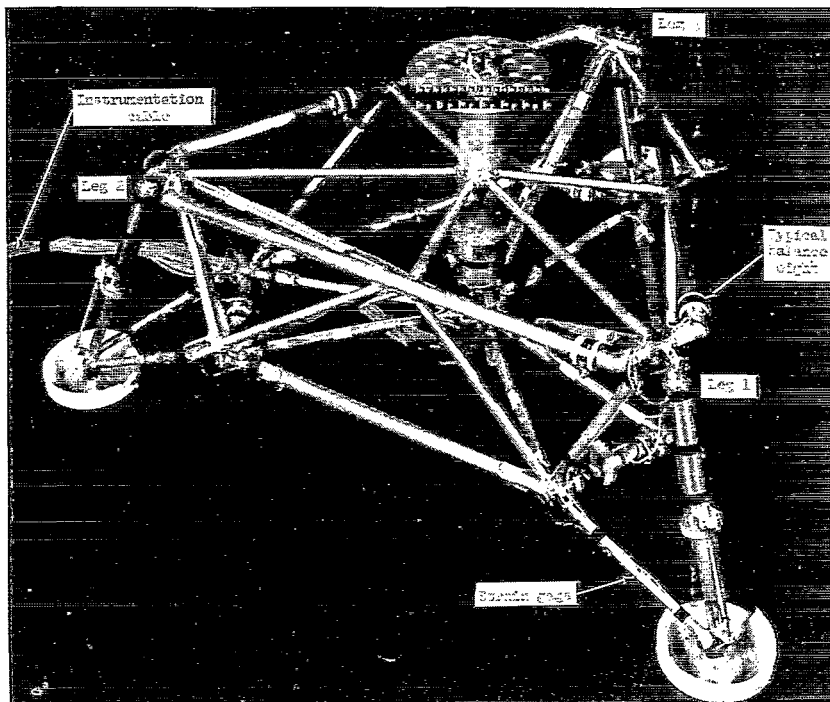


Figure 1.- General arrangement of 3/8-scale model. Dimensions are given in meters and parenthetically in inches. All values are full scale.



L-70-1775.1

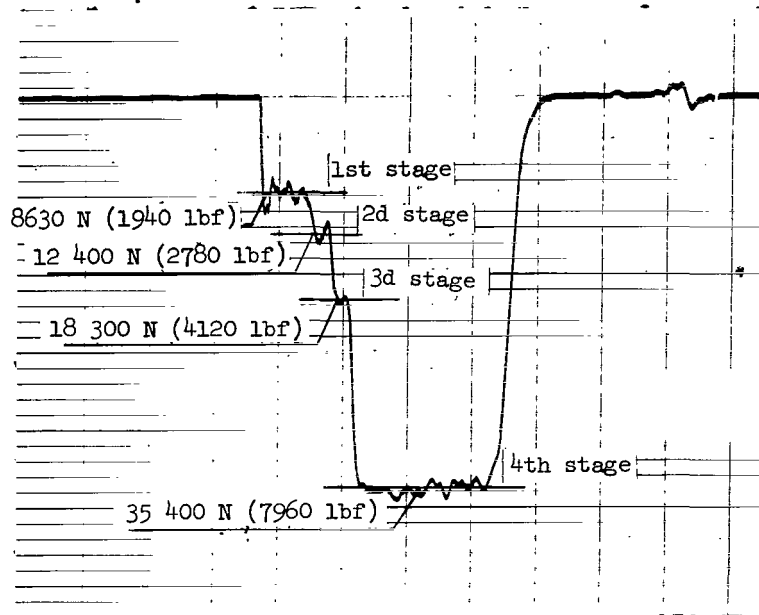
(a) Model balanced for Mars-gravity tests.



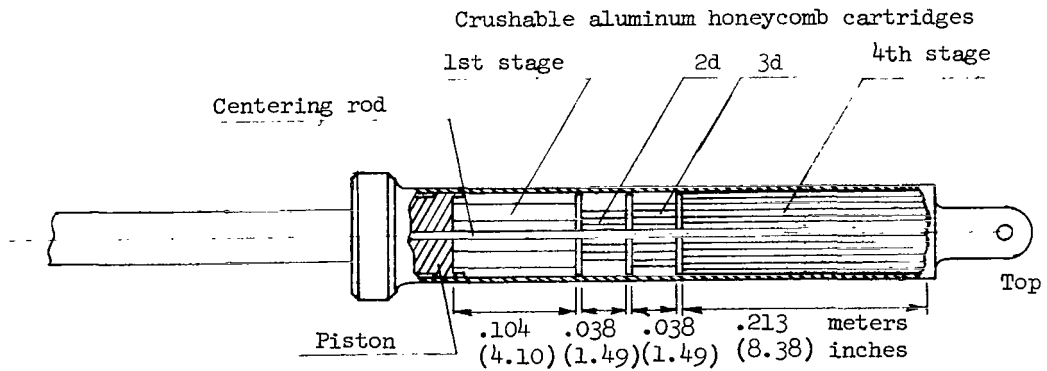
L-70-1786.1

(b) Model balanced for Earth-gravity tests.

Figure 2.- Photographs of 3/8-scale models.

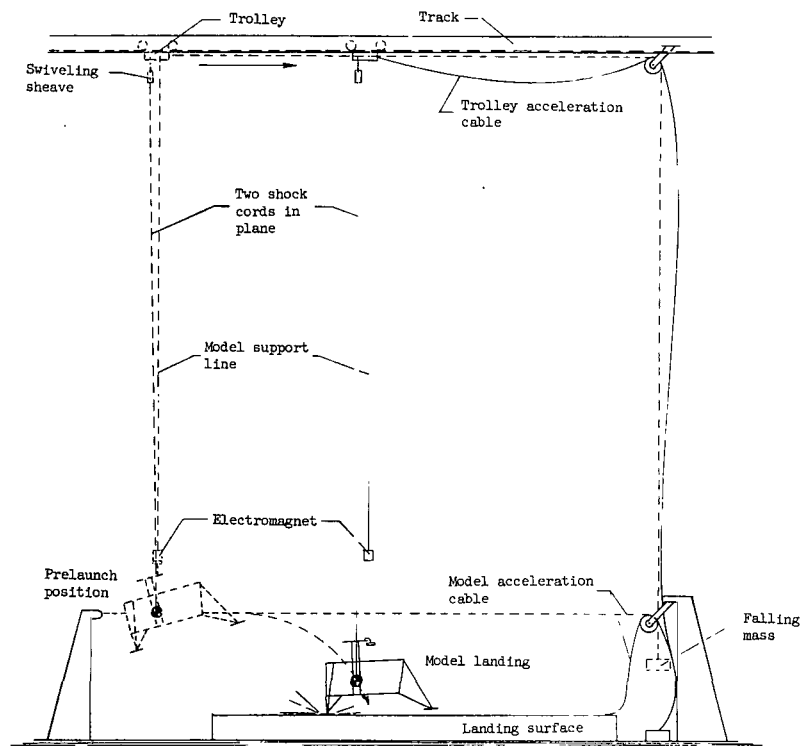


(a) Typical dynamic-force time history.

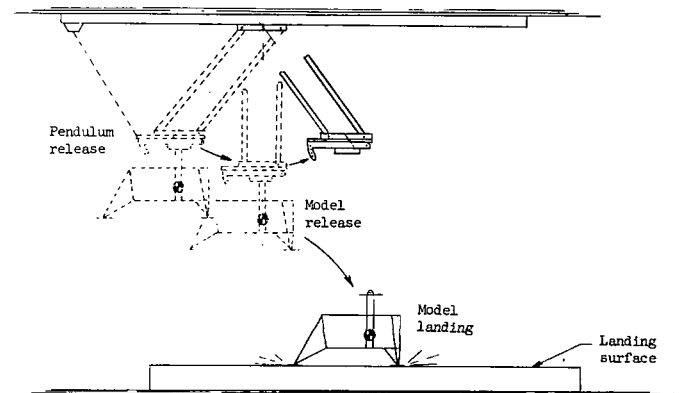


(b) Primary strut shock absorber.

Figure 3.- Primary strut shock absorber details. All values are full scale.

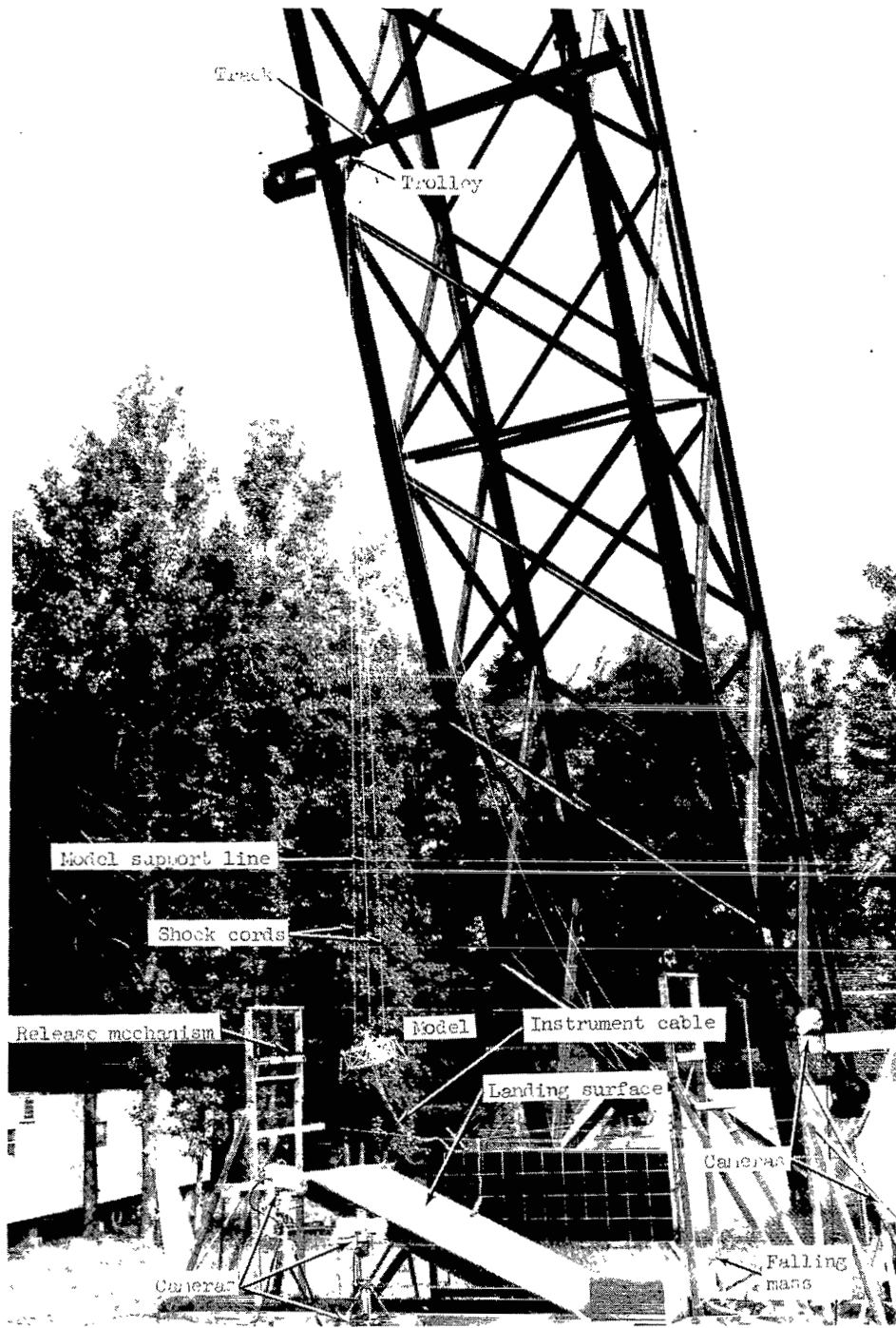


(a) Mars-gravity (elastic cord lift) simulation apparatus.



(b) Earth-gravity (free body) apparatus.

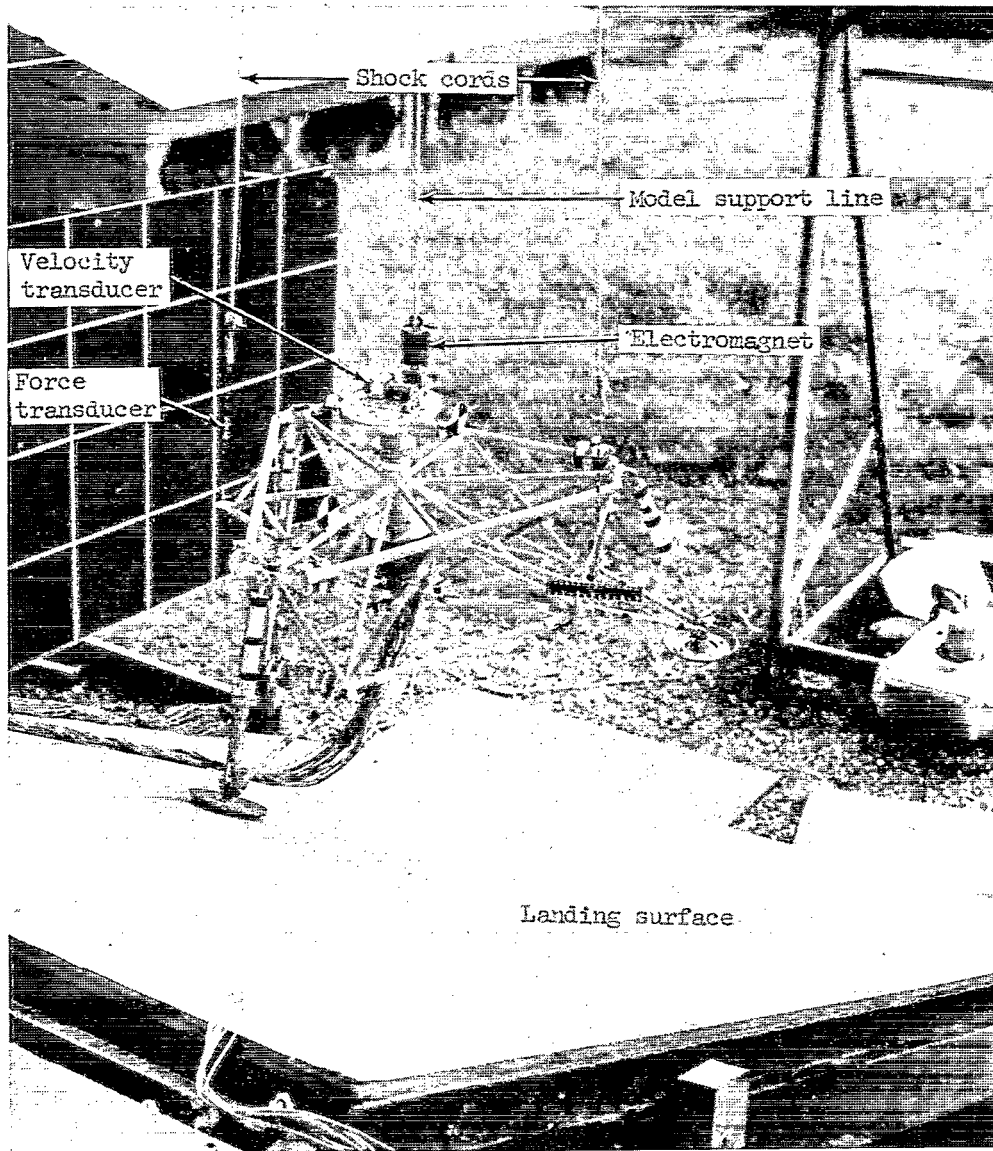
Figure 4.- Sketches illustrating launch procedure for Mars-gravity and Earth-gravity tests.



L-70-5285.1

(a) Overall view of test apparatus.

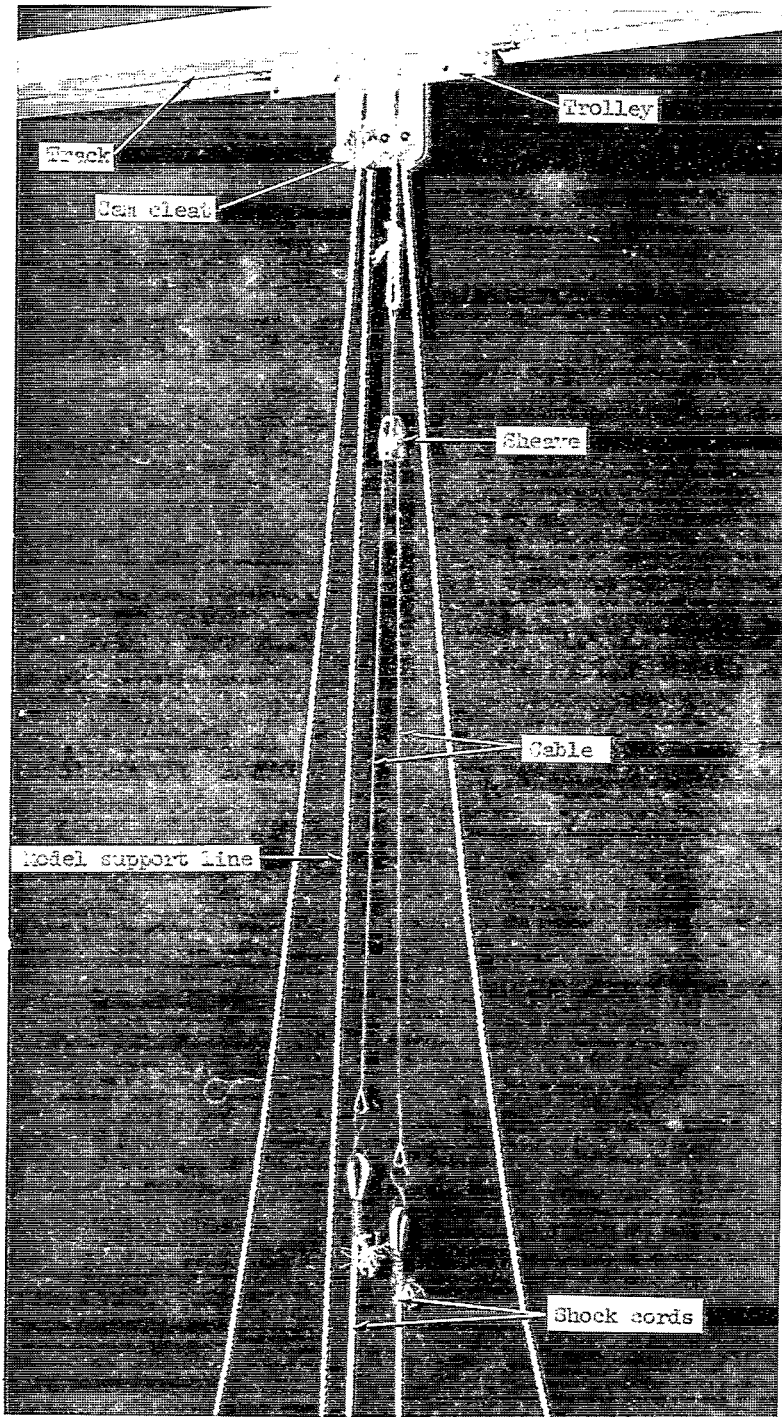
Figure 5.- Photographs of Mars-gravity simulation apparatus.



L-71-646

(b) Details of apparatus near model.

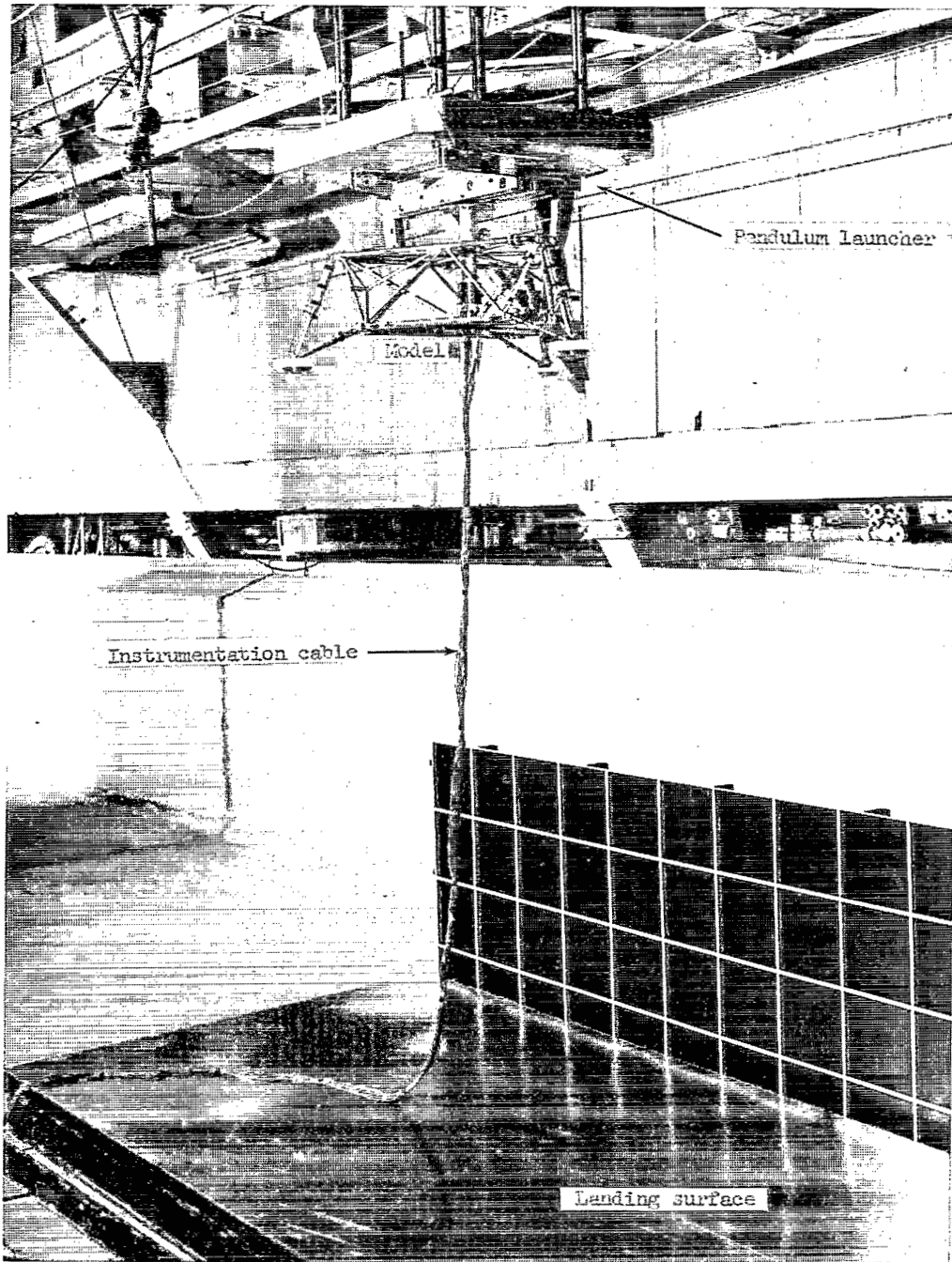
Figure 5.- Continued.



L-70-8127.1

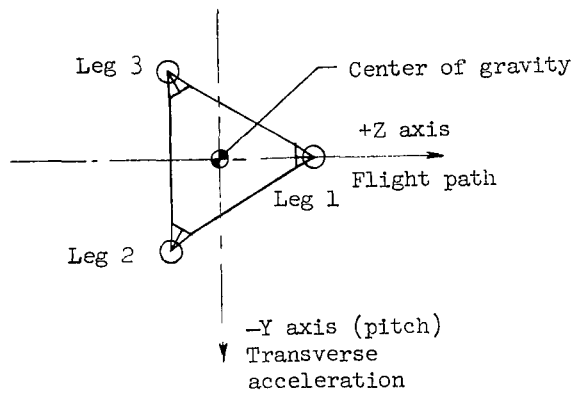
(c) Details near trolley.

Figure 5.- Concluded.



L-70-2294.1

Figure 6.- Photograph of test apparatus for Earth-gravity test.



Top view

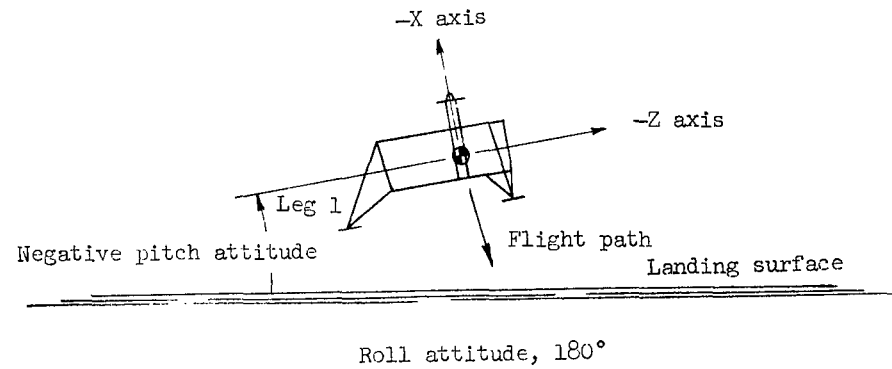
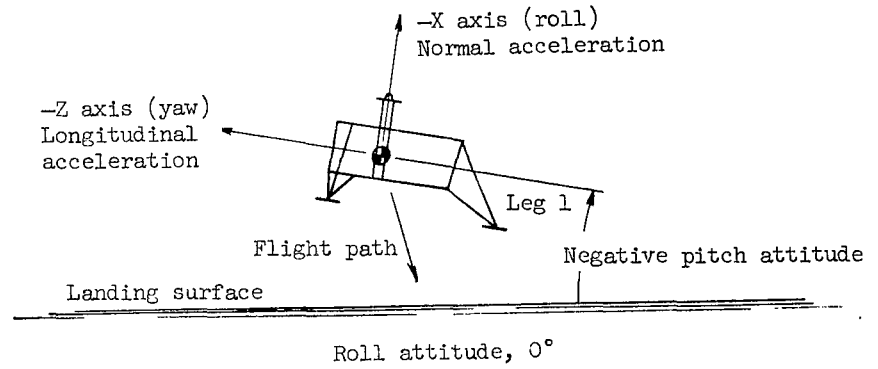


Figure 7.- Sketches identifying vehicle axes, acceleration directions, attitudes, and flight path.

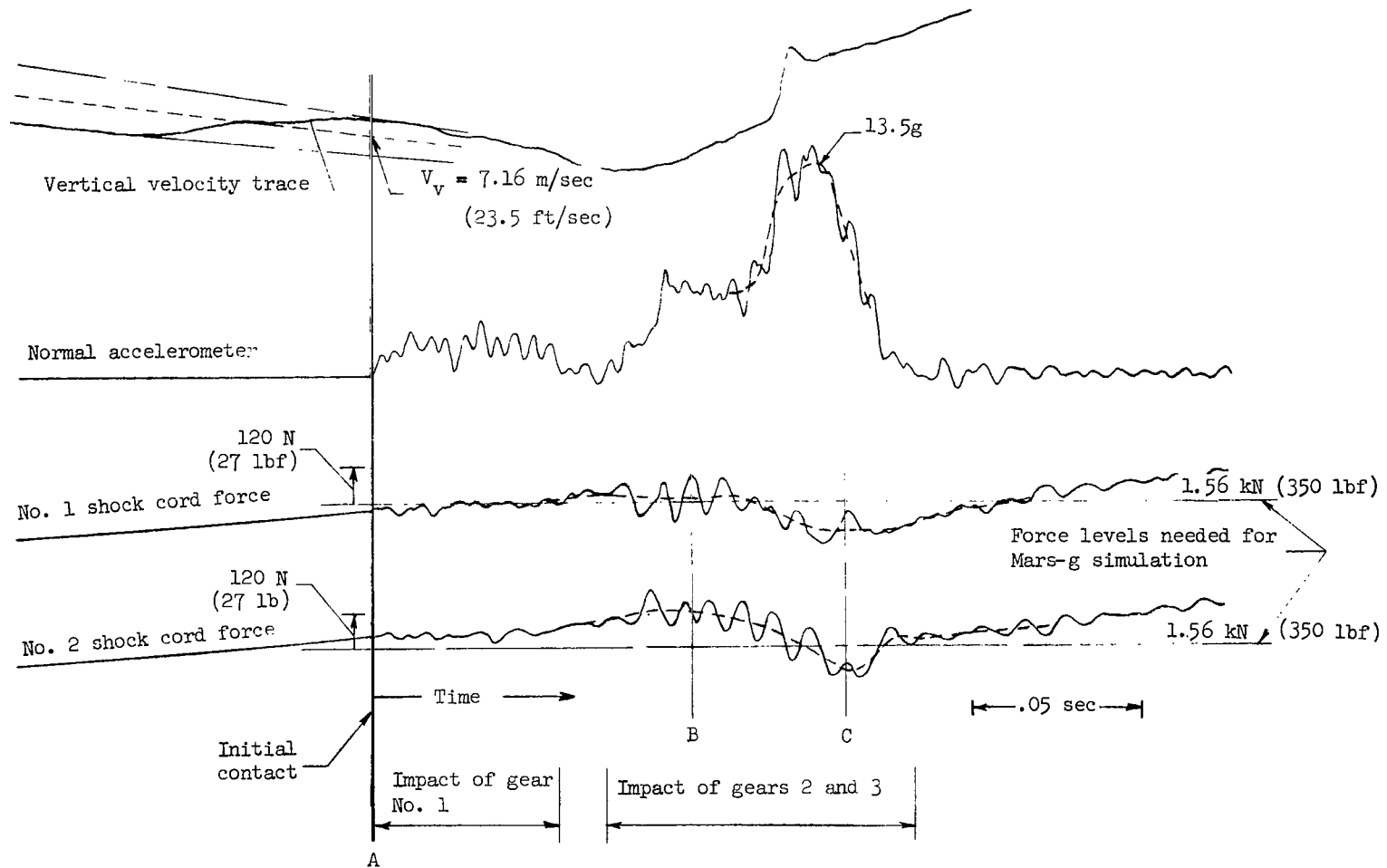
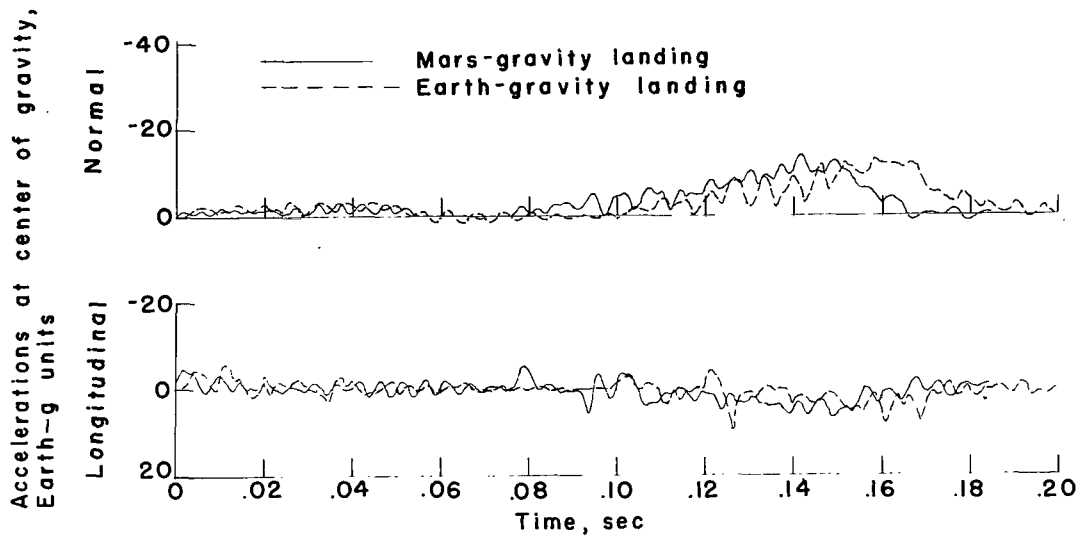
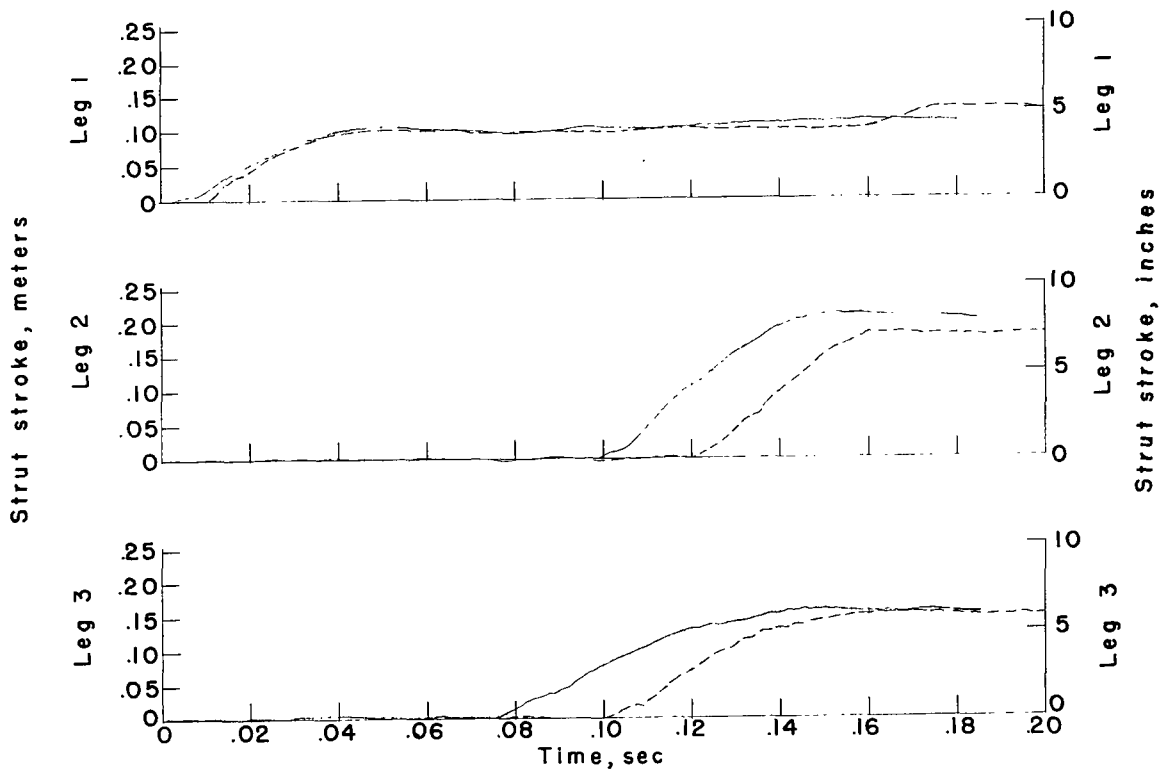


Figure 8.- Typical oscillograph record of velocity and shock cord forces. All values are full scale.

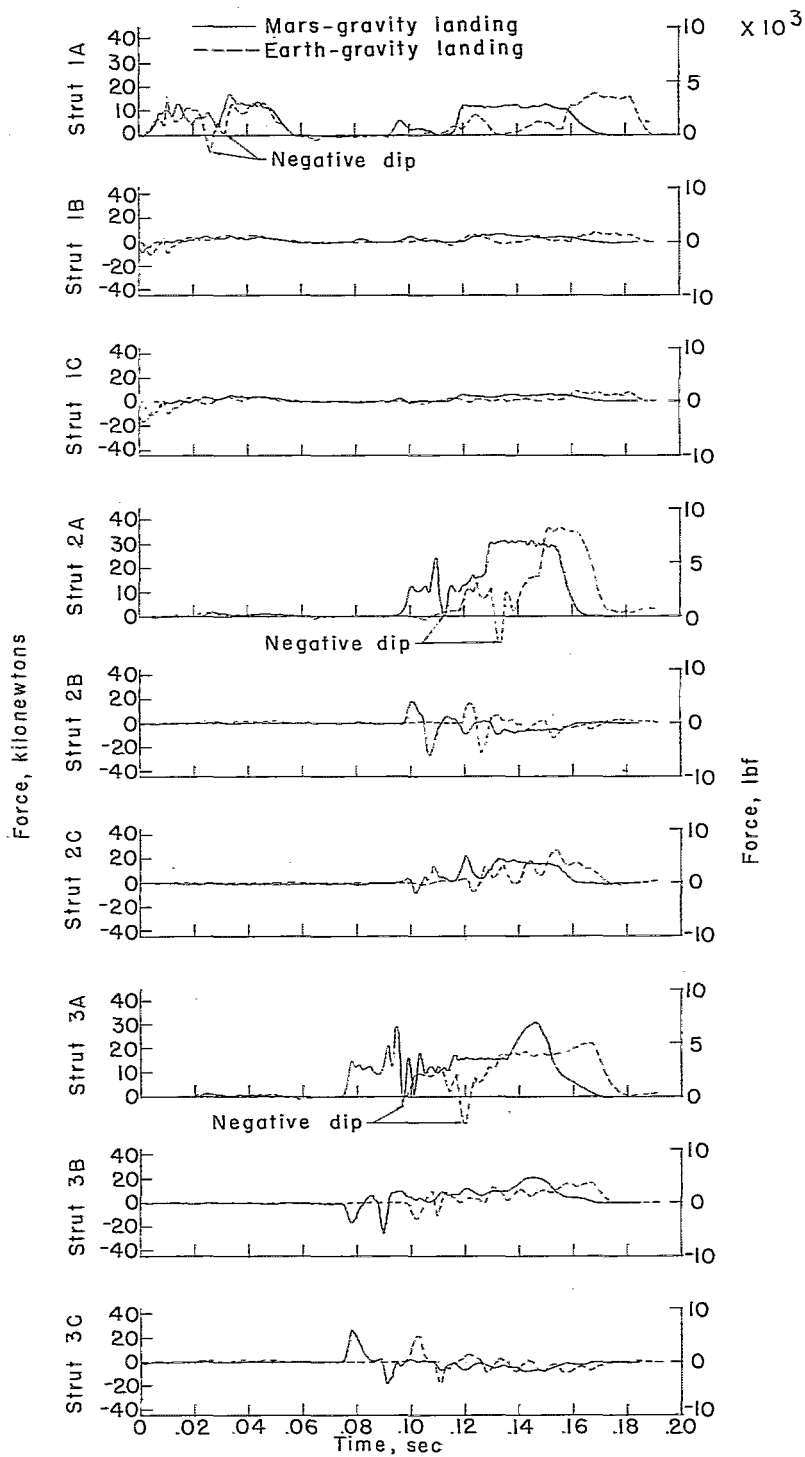


(a) Acceleration time histories.



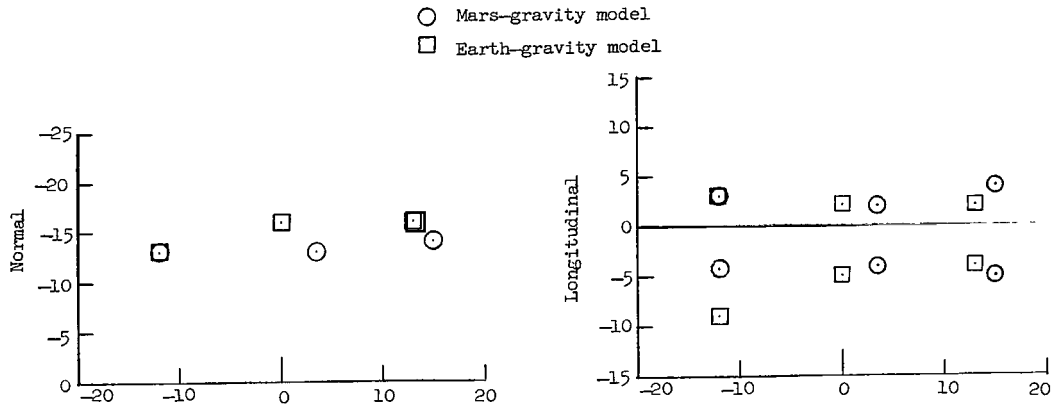
(b) Stroke time histories.

Figure 9.- Comparison of time histories obtained during landings on a smooth -20° slope with Mars-gravity and Earth-gravity models. $V_v = 7$ m/sec (23.2 ft/sec) nominal; $V_h = 2$ m/sec (6 ft/sec); pitch, 0° nominal; roll, 180° ; yaw, 2.5° left; $\mu = 0.5$. All values are full scale.

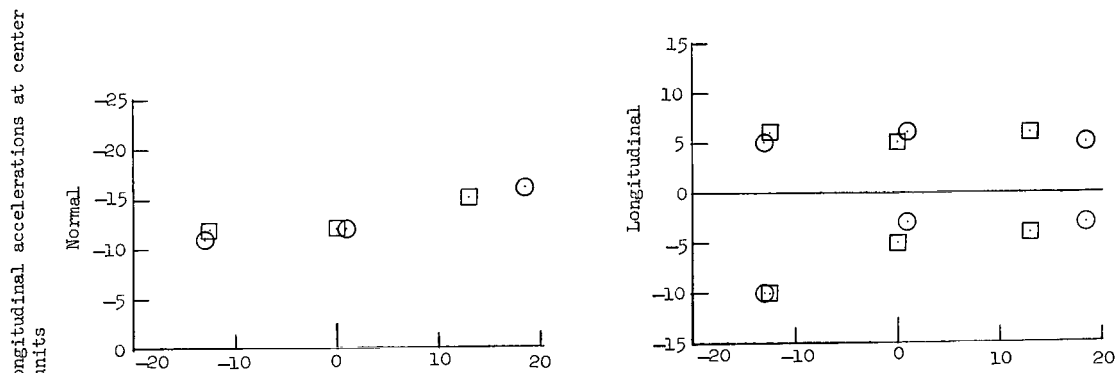


(d) Force time histories.

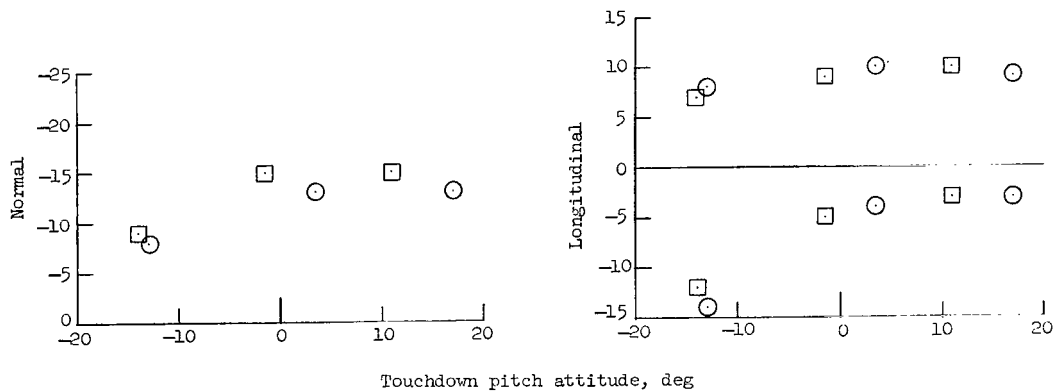
Figure 9.- Concluded.



(a) Coefficient of friction, 0.05 to 0.15.



(b) Coefficient of friction, 0.45 to 0.55.



(c) Coefficient of friction, 0.75 to 0.85.

Figure 10.- Comparison of maximum impact accelerations obtained during landings on smooth -20° slope with Mars-gravity and Earth-gravity models. $V_V = 7$ m/sec (23 ft/sec) nominal; $V_h = 2$ m/sec (6 ft/sec) nominal; roll, 180° ; yaw, 0° nominal. All values are full scale.

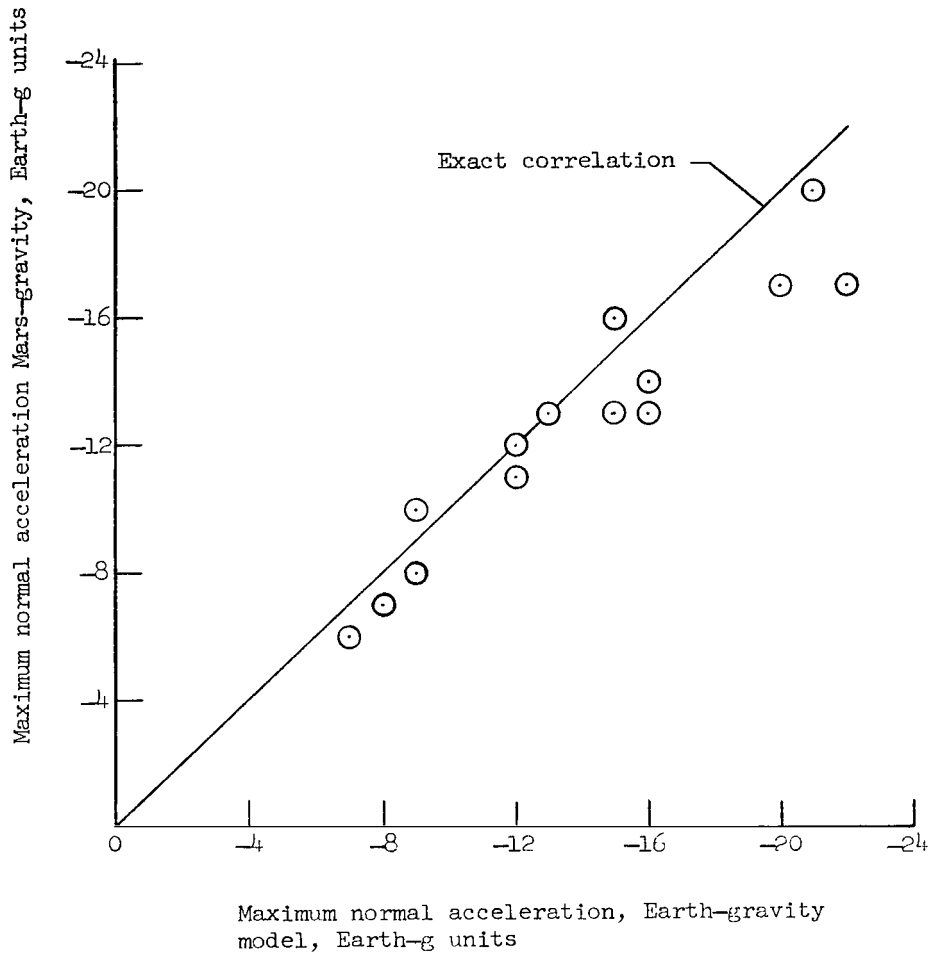


Figure 11.- Correlation of maximum normal accelerations at vehicle center of gravity for Mars-gravity and Earth-gravity landings. All values are full scale.

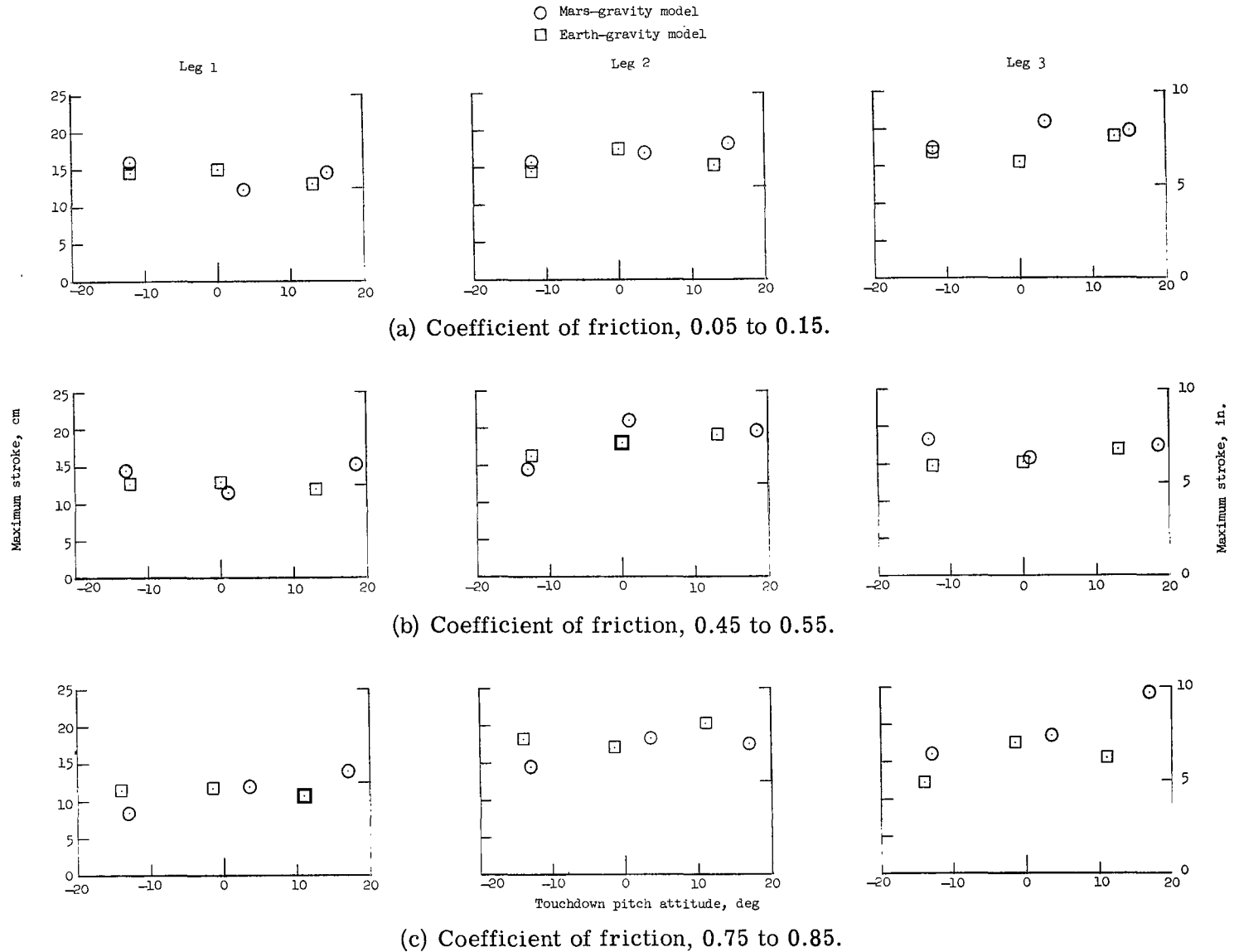


Figure 12.- Comparison of maximum landing-gear stroke obtained during landings on a smooth -20° slope with Mars-gravity and Earth-gravity models. $V_v = 7$ m/sec (23 ft/sec) nominal; $V_h = 2$ m/sec (6 ft/sec) nominal; roll, 180° ; yaw, 0° nominal. All values are full scale.

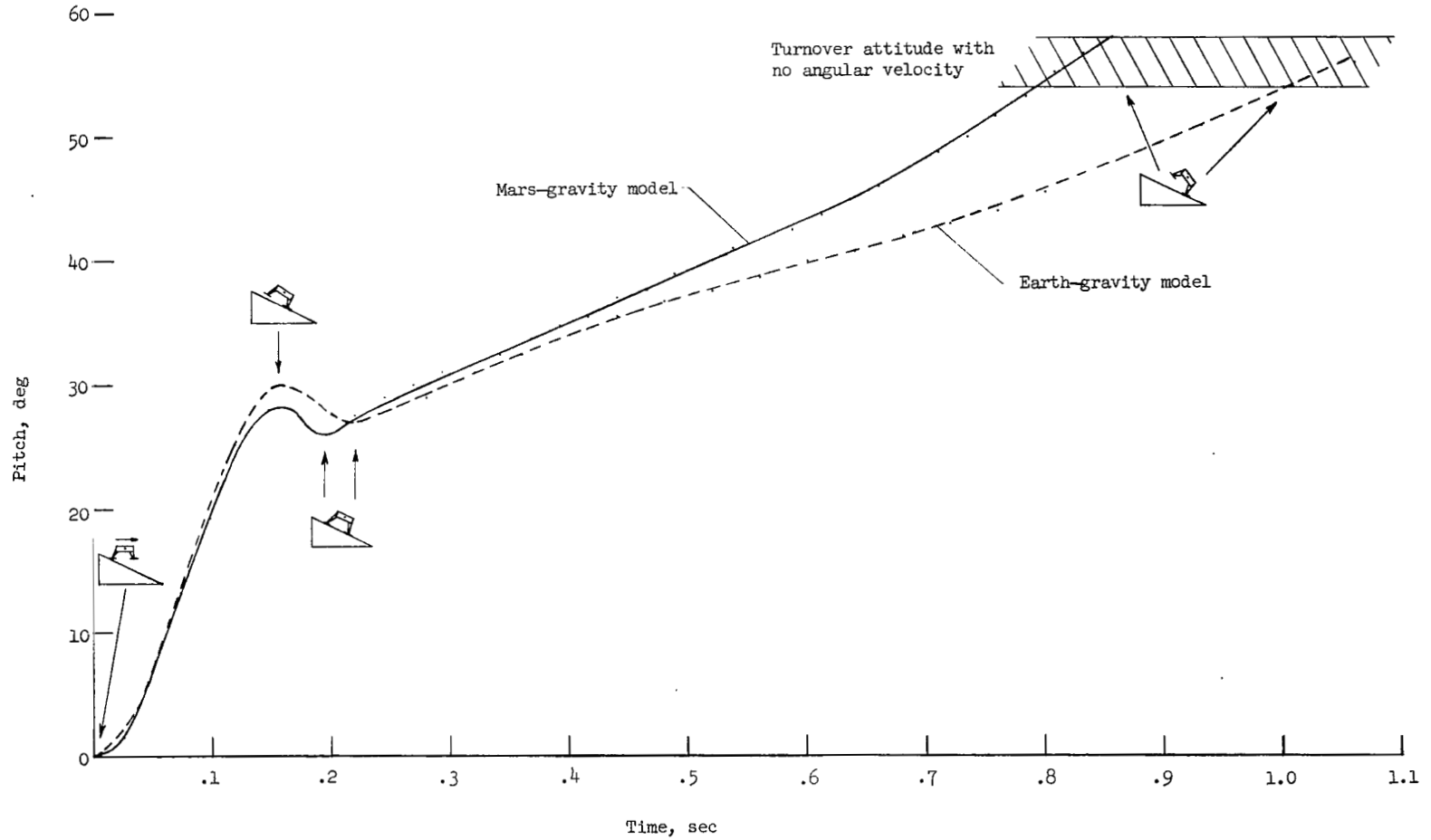


Figure 13.- Comparison of pitching motions for Mars-gravity and Earth-gravity tests. Nominal landing conditions are $V_v = 7.2$ m/sec (23.6 ft/sec); $V_h = 2$ m/sec (6 ft/sec); pitch, 0° ; roll, 180° ; yaw, 1° right; slope -25° ; and friction coefficient, 0.8. Shock-absorber forces, 36 kN (8000 lbf). All values are full scale.



018 001 C1 U 31 710917 S00903DS
DEPT OF THE AIR FORCE
AF SYSTEMS COMMAND
AF WEAPONS LAB (WLOL)
ATTN: F LOU BOWMAN, CHIEF TECH LIBRARY
KIRTLAND AFB NM 87117

POSTMASTER: If Undeliverable (Section 158
Postal Manual) Do Not Return

"The aeronautical and space activities of the United States shall be conducted so as to contribute . . . to the expansion of human knowledge of phenomena in the atmosphere and space. The Administration shall provide for the widest practicable and appropriate dissemination of information concerning its activities and the results thereof."

— NATIONAL AERONAUTICS AND SPACE ACT OF 1958

NASA SCIENTIFIC AND TECHNICAL PUBLICATIONS

TECHNICAL REPORTS: Scientific and technical information considered important, complete, and a lasting contribution to existing knowledge.

TECHNICAL NOTES: Information less broad in scope but nevertheless of importance as a contribution to existing knowledge.

TECHNICAL MEMORANDUMS: Information receiving limited distribution because of preliminary data, security classification, or other reasons.

CONTRACTOR REPORTS: Scientific and technical information generated under a NASA contract or grant and considered an important contribution to existing knowledge.

TECHNICAL TRANSLATIONS: Information published in a foreign language considered to merit NASA distribution in English.

SPECIAL PUBLICATIONS: Information derived from or of value to NASA activities. Publications include conference proceedings, monographs, data compilations, handbooks, sourcebooks, and special bibliographies.

TECHNOLOGY UTILIZATION PUBLICATIONS: Information on technology used by NASA that may be of particular interest in commercial and other non-aerospace applications. Publications include Tech Briefs, Technology Utilization Reports and Technology Surveys.

Details on the availability of these publications may be obtained from:

SCIENTIFIC AND TECHNICAL INFORMATION OFFICE

NATIONAL AERONAUTICS AND SPACE ADMINISTRATION

Washington, D.C. 20546